Key Points:

- The late morning inferred download-directed E X B drift did not support the varying equatorial ionization anomaly signature during the sudden stratospheric warming (SSW) onset
- The higher SSW effect during the mid-January was seen in the enhancement of the late morning inferred E X B drift at both hemispheres
- The slight reduction in the northern crest during the minor storm was due primarily to photo-ionization and SSW's combined effect

Correspondence to:
J. B. Fashae,
Joshua.fashae@bowen.edu.ng

Response of the Ionospheric TEC to SSW and Associated Geomagnetic Storm Over the American Low Latitudinal Sector

J. B. Fashae[1] ![ORCID], **O. S. Bolaji[1,2,3]** ![ORCID], and **A. B. Rabiu[1,4]** ![ORCID]

[1]Department of Physics and Solar Energy, Bowen University, Iwo, Nigeria, [2]Department of Physics, University of Lagos, Lagos, Nigeria, [3]Department of Mathematics and Physics, University of Tasmania, Hobart, TAS, Australia, [4]Center for Atmospheric Research, National Space Research & Development Agency, Anyigba, Nigeria

Abstract During the sudden stratospheric warming (SSW) event in 2013, we investigated the American low latitude around 75°W. We used 12 Global Positioning System (GPS) receivers, a pair of magnetometers, and the NASA Thermosphere Ionosphere Mesosphere Energetics and Dynamics (TIMED) satellite airglow instrument to unveil the total electron content (TEC), inferred vertical drift, and the changes in the neutral composition, respectively. A major SSW characterized the 2013 SSW event with the main phase (7–27 January 2013) overlapped by a minor geomagnetic storm (17 January 2013). The late morning inferred downward-directed E X B drift did not support the varying equatorial ionization anomaly (EIA) signature during the SSW onset (7 January 2013). The mid-January (15–16 January 2013) witnessed enhancement in the varying inferred upward-directed E X B drift at both hemispheres. On 17 January 2013, there were reductions in the varying inferred upward-directed E X B drift at both hemispheres. Generally, the SSW effect on TEC around 15–16 January 2013 is more pronounced than the SSW onset. During the mid-January (15–16 January 2013), the higher northern EIA crests are facilitated majorly by the SSW compared to the photo-ionization that primarily enabled the southern crests. On 17 January 2013, the combined effect of photo-ionization and SSW contribution was majorly responsible for the slight reduction in the northern crest. In the southern hemisphere, photo-ionization played the lead role as the SSW, and the minor geomagnetic storm roles are secondary in enhancing the southern crest.

Plain Language Summary The vertical coupling between the lower atmosphere and the ionosphere is evident during large-scale metrological events called sudden stratospheric warming (SSW). This event occurred during the northern wintertime and was characterized by the sudden breakdown of the stratospheric polar vortex due to the enhanced amplitude of the upward propagating planetary waves in the stratosphere. We investigated the American low-latitude ionosphere during 2013 SSW and when overlapped by a minor geomagnetic storm using total electron content (TEC) data from Global Positioning System receivers. A pair of magnetometers and the NASA Thermosphere Ionosphere Mesosphere Energetics and Dynamics satellite airglow instrument revealing the varying vertical inferred E X B drift and global changes in the neutral composition, O/N_2 ratio are also used. The late morning inferred downward-directed E X B drift during the SSW onset did not support the varying EIA signature. The re-location of the northern equatorial ionization anomaly (EIA) crest during mid-January was associated with an enhancement in the variable semidiurnal late morning inferred upward-directed drift due to intensified SSW conditions. The combined effect of the photo-ionization and SSW caused a slight reduction of the TEC at the northern crest during the ongoing SSW modulated by a minor storm.

1. Introduction

A daytime production of photo-ionization associated with solar extreme ultra-violet (EUV) radiation increases electron density at all the latitudes as discussed by Rishbeth et al. (2000) using solar radio flux as a proxy for solar EUV. In addition to photoionization during quiet geomagnetic conditions, the varying atmosphere neutral wind modulated electron density across all latitudes (Balan et al., 2018). Compared to the high and middle latitudes, the equatorial and low-latitude ionosphere is also strongly associated with a transport process characterized by the equatorial electrojet (EEJ) strength, fountain effect and equatorial ionization anomaly (EIA). During the quiet conditions, the magnetic equator's daytime zonal electric field (EEJ strength) generated by wind dynamo

mechanism gets mapped into F-region through the magnetic field lines. This creates a vertical upward-directed EXB drift that is responsible for removing plasma around the dip equator to higher altitudes as the new ionosphere develops at the lower altitudes (Balan et al., 1998). After losing momentum due to the force of gravity and electron density gradient, the uplifted plasma diffuses along the magnetic field lines to higher altitude on both sides of dip equator; a process called fountain effect (Balan & Bailey, 1995; Hanson & Moffet, 1966). This transport process led to a crest being formed on both sides of the low latitude and reduced the ionosphere plasma around the magnetic equator. This combined signature is referred to as equatorial ionization anomaly (EIA).

The magnetosphere-ionosphere coupling during a geomagnetic storm is a space weather event, which is generally referred to as forcing from above the ionosphere. During the magnetosphere-ionosphere coupling, almost all the atmosphere latitudes are modulated (Fuller-Rowell et al., 1994; Richmond & Lu, 2000). This is attributed to different large-scale physical processes like changes in the storm-time neutral atmospheric composition, the prompt penetration of electric field (PPEF), the ionospheric disturbance dynamo electric field (DDEF), solar heating, and thermospheric winds (Blanc & Richmond, 1980; Fuller-Rowell et al., 1994, 1996; Gonzales et al., 1979; Nishida, 1968; Vasyliunas, 1970, 1972). It is important to note that the varying storm-time equatorward wind and PPEF in the low latitudes that enhanced the EIA features (Tsurutani et al., 2008) and modulated it to an equatorial peak (Bolaji et al., 2021) can cause a more complex variability of the equatorial and low-latitude electrodynamics (Venkatesh et al., 2017).

It is also important to note that, besides the well-known ionospheric variabilities associated with space weather events such as geomagnetic storms, recent studies have shown that daily ionospheric variabilities can also be induced by sudden stratospheric warming (SSW) events during winter seasons (Forbes, 2000; Laštovička, 2006; Goncharenko, Chau, et al., 2010; Goncharenko, Coster, et al., 2010; Liu et al., 2013). SSW event is a meteorological phenomenon related to a rapid increase of the polar stratosphere temperature for several days during the northern winter. During this period, the zonal mean zonal wind that propagates westward decelerates (minor warming) or reverses to eastward (major warming) and interact non-linearly with the planetary wave (PW), resulting in the upward propagating waves toward the mesosphere lower thermosphere (MLT) region (Matsuno, 1971; Meyer Christian, 1999). Energy and momentum transfer due to SSW events modulate the vertical ions drift (Anderson & Araujo-Pradere, 2010; Chau et al., 2009; Fejer et al., 2010, 2011; Lin et al., 2012), equatorial electrojet (Bolaji et al., 2016; Yamazaki et al., 2012), and total electron content, TEC in the ionosphere (Bolaji et al., 2017, 2019; Chau et al., 2010; De Jesus et al., 2017; Fagundes et al., 2016; Goncharenko, Chau, et al., 2010; Liu et al., 2011; Korenkov et al., 2012; Paes et al., 2014).

A better understanding of the ionosphere response to SSW events that have remained one of the ongoing frontrunners about space weather is the key aim of this study. For example, the January 2013 SSW event (7 January–27 January 2013) is peculiar because it was characterized by long-lasting major SSW event. On 7 January 2013, the major SSW conditions were satisfied (SSW onset). According to the World Meteorological Organization (WMO) standard, a major SSW occurs when the stratospheric temperature at the northern polar region increased more than 25 K within a week and the westward-directed stratospheric zonal mean zonal wind turns eastward.

The major SSW recovered briefly on 10 January 2013 (relaxing SSW) when the variable zonal mean zonal wind reversed westward by excursing a positive value of 1.6 m/s and a slight reduction in the varying stratospheric temperature was noticeable (shown with red circles, Figure 2a and 2b). Thereafter, the major SSW was again seen around 12 January 2013 until around 27 January 2013 when recovery phase started. However, on 17 January 2013, the ongoing major SSW was modulated by a minor geomagnetic storm. Maute et al. (2015) had investigated the same 2013 SSW in the American sector, focusing more attention around 15–20 January 2013 as it was modulated by a moderate storm on 17 January 2013.

Except for Maute et al. (2015), Hagan et al. (2015), Pedatella et al. (2016) and Pedatella and Liu (2018) that used numerical simulations to investigate the combined effects of geomagnetic and meteorological activities on the ionosphere, the majority of earlier studies, especially in January 2013 were reported discretely. For instance, Goncharenko et al. (2013) and Jonah et al. (2014) studied the ionospheric effect of the 2013 SSW events over American low-latitude region using the GPS-TEC data. They reported strong perturbations in the TEC value at the crests of EIA compared to the background value and attributed it to the anomalous variations in vertical ion drift. Ribeiro et al. (2019) also used GPS-TEC data over the American sector to investigate the response of equatorial and low-latitudes positive ionospheric phases due to moderate geomagnetic during high solar activity

Table 1
Details of Global Positioning Systems (GPS) Station Names, Station Codes, Geographic and Geomagnetic Longitudes and Latitudes

	Station location	Country	Station codes	Geographical coordinates	Geomagnetic coordinates
1.	Magangue	Colombia	VMAG	9.29°N, 74.85°W	21.43°N, 357.56°W
2.	Bogota	Colombia	BOGT	4.71°N, 74.07°W	16.93°N, 358.11°W
3.	Esmeraldas	Ecuador	ESMR	0.96°N, 79.65°W	13.02°N, 351.56°W
4.	Puengasi	Ecuador	QUEM	0.24°S, 78.49°W	11.96°N, 352.82°W
5.	Pucallpa	Peru	LPUC	8.38°S, 74.57°W	4.25°N, 356.88°W
6.	Huancanyo	Peru	IHYO	12.04°S, 75.32°W	0.63°N, 356.08°W
7.	Galeras	Peru	GLRV	14.67°S, 74.40°W	1.89°S, 357.01°W
8.	Arica	Chile	IACR	18.47°S, 70.33°W	5.58°S, 0.70°W
9.	Antofagasta	Chile	VCNF	23.68°S, 70.41°W	10.58°S, 0.58°W
10.	Copiapo	Chile	COPO	27.38°S, 70.33°W	14.10°N, 0.69°W
11.	Valparaiso	Chile	VALN	33.02°S, 71.63°W	19.38°S, 359.97°W
12.	Talcahuano	Chile	CONZ	36.84°S, 73.02°W	22.96°S, 359.34°W

in January 2013. They revealed significant changes in the electrodynamics of the ionosphere during the storm's main and recovery phases and attributed them to the traveling ionospheric disturbance (TID).

Although, these investigations have enlarged our scope of understanding about the SSW effect on the ionosphere on one side and the minor geomagnetic storm effect on another side. Most significantly, the effort of Maute et al. (2015) is acknowledged as they used vertical drift observations and the National Center for Atmospheric Research (NCAR) thermosphere-ionosphere-mesosphere electrodynamics general circulation model (TIME-GCM) to investigate ongoing major SSW that was modulated by a moderate geomagnetic storm on 17 January 2013. On this day, they observed an enhancement in the daytime vertical drift compared to 22 January 2013 (a non-SSW day) and attributed it to 50% contribution, each from SSW and a moderate geomagnetic storm effect. On the SSW effect, the increase in the wind dynamo leading to enhancement in the daytime vertical drift was attributed to the migrating solar and semidiurnal westward propagating tides. The moderate geomagnetic storm effect was attributed to an increase in daytime vertical drift due to prompt penetration electric field (PPEF).

Despite these efforts, it is still unclear to the space weather community how this vertical drift characterized by a combined effect of an ongoing major SSW and minor geomagnetic storm on 17 January 2013 modulated the equatorial ionization anomaly (EIA) signature from GPS TEC observations. We will compare the effect of the SSW onset on 7 January 2013 and around 15–16 (mid-January) on the EIA signatures and discuss the interplay of photo-ionization, SSW and geomagnetic storm forcing that could be responsible for such changes. In addition, this study will demonstrate to the space weather community and document the contributions of the inferred vertical drift, photo-ionization, SSW and the minor geomagnetic storm effects to the low latitude crests.

2. Data and Methodology

Table 1 shows the list of station names, their codes, geographic and geomagnetic coordinates of the TEC data employed over 12 low-latitude stations along the American longitudes (Figure 1). The GPS TEC data were retrieved from cddis.nasa.gov/archive/gnss/data/. More details on GPS TEC analysis have been given in the works of Goncharenko, Coster, et al. (2010) and Bolaji et al. (2012).

Figure 2 shows the varying stratospheric temperature, zonal mean zonal wind, solar flux, Kp index, IMF Bz and SYM-H during the months of December 2012–February 2013 in panels a, b, c, d, and e, respectively. The stratospheric temperature started increasing significantly on 4 January 2013 (210 K) and reached its peak (239.9 K) on 7 January 2013 (shown between vertical red and green lines, Figure 2a). This corresponds to more than 25 K increase in the stratospheric temperature at 10 hPa within a week from 1 January to 10 January 2013 (Maute et al., 2015). Coincidentally, on this same day of stratospheric temperature peak, the varying zonal mean zonal wind at 60°N and 10 hPa turned eastward (shown in Figure 2b). These indicate an ongoing major sudden
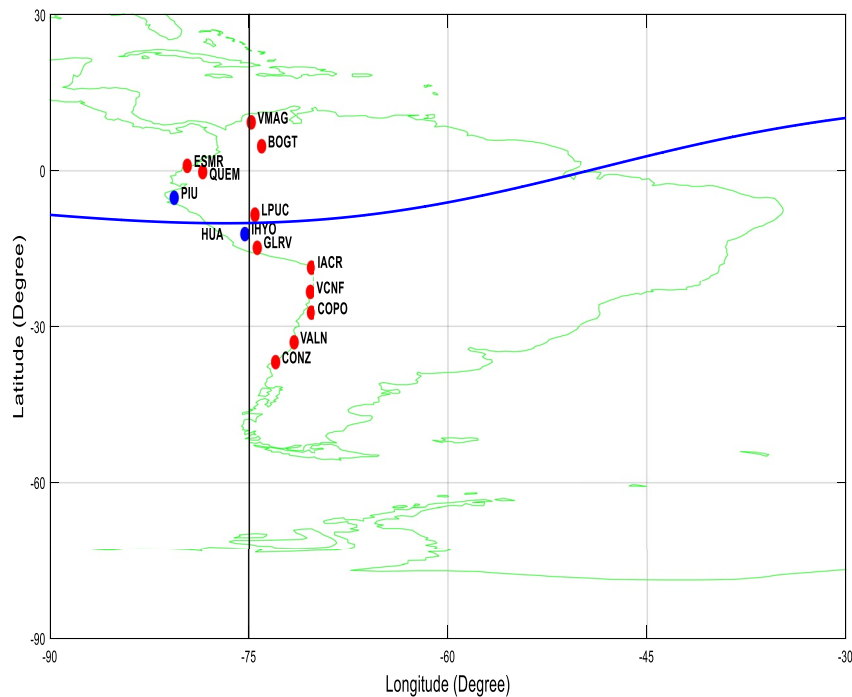
Figure 1. A map showing the American low latitude Global Positioning System stations used in this investigation.

stratospheric warming, SSW. After the peak in stratospheric temperature, a downward progression began and lasted for about 3 days. Also, the stratospheric zonal mean zonal wind was reversed to a positive value of 1.6 m/s on 10 January 2013, indicating a minor recovery from a major SSW period. The long-lasting SSW main phase continues on 12 until 27 January 2013, with the zonal mean zonal wind reaching a maximum of −12 m/s on 18 January 2013. During the ongoing major SSW, a minor geomagnetic storm with SYM-H of ∼−58 nT modulated it on 17 January 2013 (indicated by blue dotted lines). Around this period, the varying southward-directed IMF Bz reached ∼−15 nT. The January 2013 SSW event coincided with the varying F10.7 in the range of 110 sfu–168 sfu.

Figures 3–5 also indicate the stratospheric, solar, and geomagnetic parameters during the 2011/2012 (when $F_{10.7}$ = 140 sfu), 2013/2014 (when $F_{10.7}$ = 168.2 sfu), and 2012/2013 (when $F_{10.7}$ = 120 sfu) SSW events (indicated by vertical dashed brown, blue and black lines) respectively, 1sfu = $10^{-22} Wm^{-2} Hz^{-1}$. These solar flux periods are regarded as quiet conditions for each of the specified solar flux values while other parameters are minimal. The stratospheric parameters consisting of the zonal mean zonal wind (60°N) and stratospheric temperature (90°N) at 10 hPa (∼32 km altitude) were retrieved from the NOAA Physical Sciences Laboratory at https://psl.noaa.gov/. This is used to study the influence of meteorological forcing on different current systems in the ionosphere. Further details regarding the NCEP-NCAR reanalysis data can be found in Kalnay et al. (1996). While, the geomagnetic (SYM-H and Kp), and solar (F10.7, IMF Bz) conditions were also obtained from the NASA OMNIweb service, https://omniweb.gsfc.nasa.gov/, and the National Oceanic and Atmospheric Administration (NOAA) solar data service at https://www.ngdc.noaa.gov/stp/solar/solardataservices.html. The neutral composition, thermospheric O/N_2 column density data is optically obtained from NASA Thermosphere Ionosphere Mesosphere Energetics and Dynamics satellite (TIMED/GUVI) Far Ultraviolet (FUV) airglow instruments at http://guvitimed.jhuapl.edu.

The GPS-TEC data obtained were used to calculate the vertical total electron content (VTEC). The EIA variability from VTEC was displayed in Figures 6a–6c and 7a–7b during the non-SSW (01–31 December 2012) and SSW periods (01–20 January 2013), respectively.

Figures 9a–9c depicts the corresponding daily TEC variability due to the specified solar flux effect mentioned above (Figures 3–5). For instance, the above solar flux values correspond to the solar flux value during major SSW onset (when $F_{10.7}$ = 140 sfu), significant recovery from major SSW (when $F_{10.7}$ = 168 sfu) and mid-January
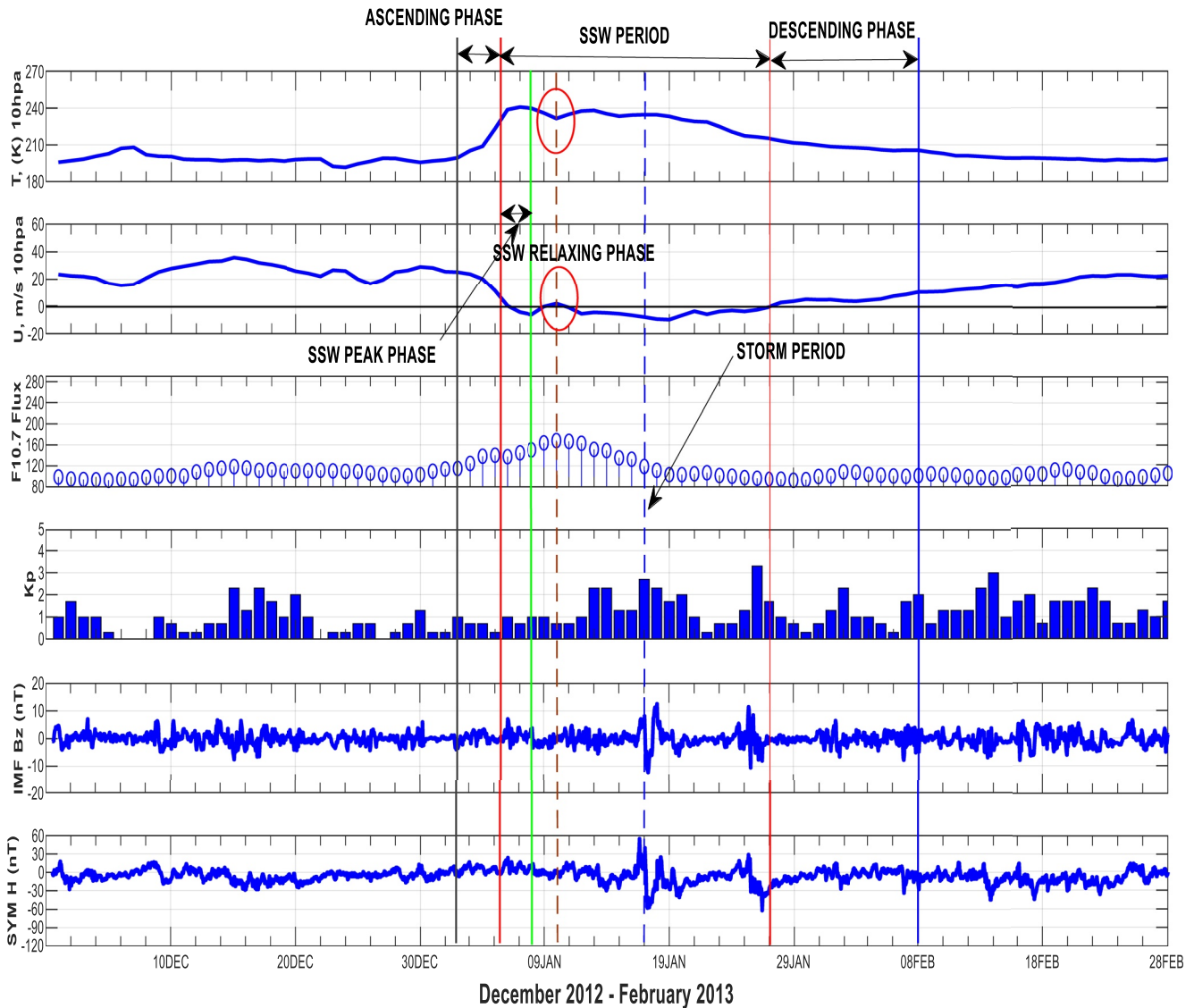
Figure 2. The stratospheric, solar, and geomagnetic parameters during December 2012–February 2013 sudden stratospheric warming (SSW) events. The two vertical solid red lines and dashed blue line indicate the peak of the SSW events and the period of minor the geomagnetic storm, respectively.

period (when $F_{10.7}$ = 119.8 sfu) (Figure 2c). The corresponding TEC values due to the specified solar flux effect as shown in Figures 9a–9c are averaged and denoted by TECquiet (TECquietave$_{(F10.7)}$). Hence, during the SSW onset (7 January 2013), we deduced the contributions of SSW (TEC$_{(SSW)}$) to the varying TEC by subtracting the TECquietave$_{(F10.7)}$ in January 2012 (Figure 9a, when $F_{10.7}$ = 140 sfu) from the TEC variations due to the SSW onset and the specified solar flux (TEC$_{(SSW + F10.7)}$, Figure 7a). A similar approach was used to estimate the SSW contributions to the varying ionospheric TEC during the relaxing SSW phase (10 January 2013, Figure 9b) and the mid-January period (15 and 16 January 2013, Figure 9c). The station by station line plots of the SSW contribution during the SSW onset, relaxing SSW phase and mid-January period of SSW are shown in Figures 10a–10c respectively. On 17 January 2013 that included major SSW, $F_{10.7}$, and a minor geomagnetic storm (TEC$_{(SSW + F10.7+STORM)}$), the contribution of the $F_{10.7}$ (regarded as TECquiet when $F_{10.7}$ = 120 sfu, Figure 9b) was deducted leaving the contribution of SSW and a minor geomagnetic storm (TEC$_{(SSW + storm)}$). Thereafter, the contribution of a minor geomagnetic storm (TEC$_{(STORM)}$) to the ongoing SSW-induced TEC was deduced by subtracting the SSW contribution (TEC$_{(SSW)}$) on 16 January 2013 (as shown in Figure 10c and 10d) from TEC$_{(SSW + storm)}$ on 17 January 2013 (Figure 10c and 10d). All of these are mathematically expressed as follow:
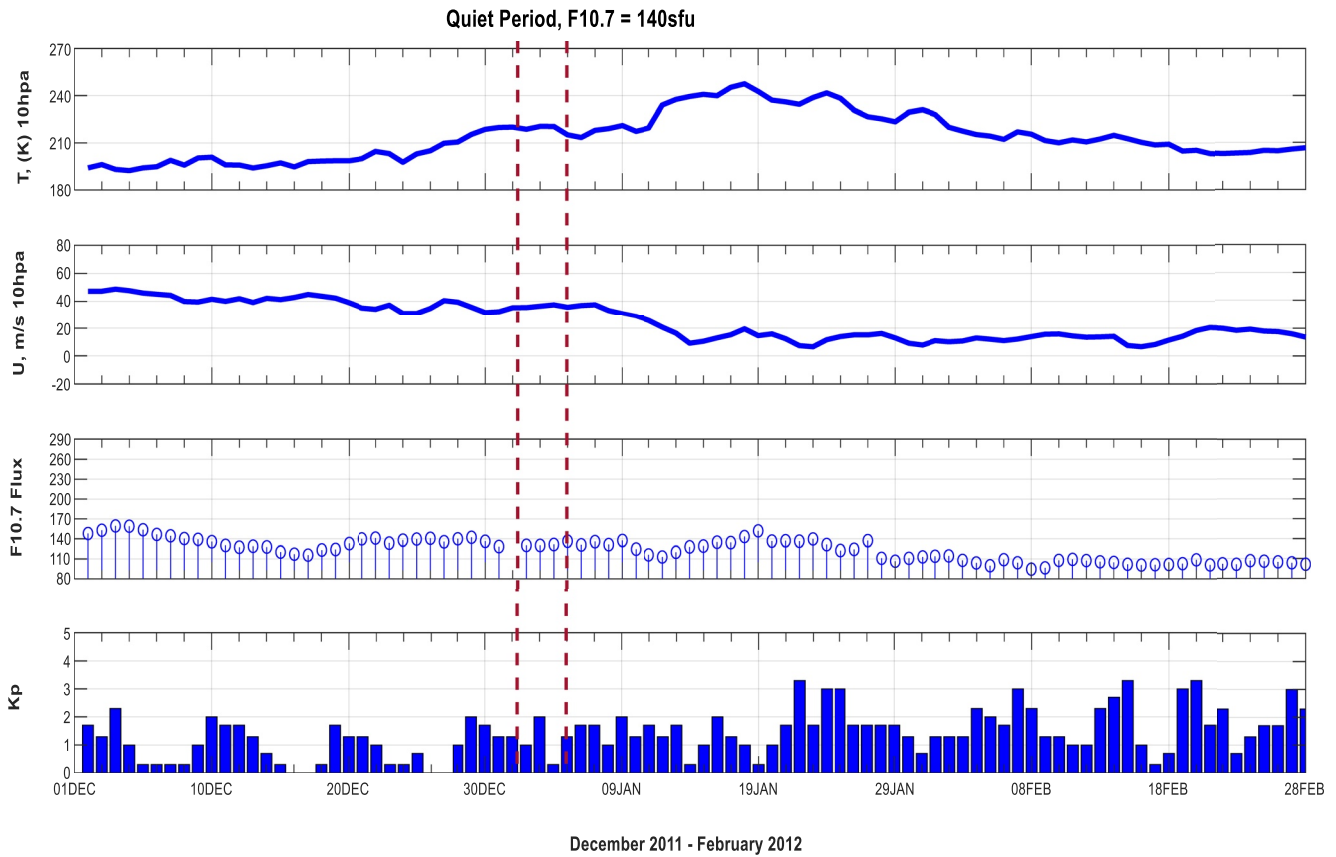
Figure 3. The stratospheric, solar, and geomagnetic parameters during December 2011–February 2012 sudden stratospheric warming events. The two vertical dashed brown lines indicate the period when solar flux, $F_{10.7}$ = 140 sfu (2–4 January 2012).

$$TEC_{(SSW)} = TEC_{(SSW+F10.7)} - TECquietave_{(F10.7)} \qquad (1)$$

$$TEC_{(SSW+STORM)} = TEC_{(SSW+F10.7+STORM)} - TECquietave_{(F10.7)} \qquad (2)$$

$$TEC_{(STORM)} = TEC_{(SSW+STORM)} - TEC_{(SSW \; on \; 16 \; January \; 2013)} \qquad (3)$$

More so, percentage contribution of the storm and SSW is as follow:

$$\% \, TEC_{(SSW)} = \frac{TEC \, (SSW)}{TEC \, (SSW + STORM)} * 100 \qquad (4)$$

$$\% \, TEC_{(STORM)} = TEC_{(SSW+STORM)} - \% \, TEC_{(SSW)} \qquad (5)$$

Conclusively, the individual contribution effect of SSW, solar flux and geomagnetic storm during the 2013 major SSW events are shown in Table 2.

3. Results and Discussion

Figures 6a–6c and 7a–7b show the day-to-day EIA variations of TEC in the American low-latitude ionosphere around 75°W during non-SSW (01–31 December 2012) and SSW periods (01–20 January 2013), respectively. The northern EIA crest, QUEM (11.96°N) that was poleward during the non-SSW period (Figure 6a) moved equatorward to LPUC (4.25°N) during SSW periods (Figure 7a). Compared to the southern hemisphere, the southern crests seen at IACR (5.58°S) remained unchanged during both the non-SSW and SSW periods. In addition to the SSW and other electrodynamics processes responsible for 7, 9, 10 and 14–17 January 2013 that will be extensively discussed, later on, the equatorward drifts of the northern crest during the SSW period are
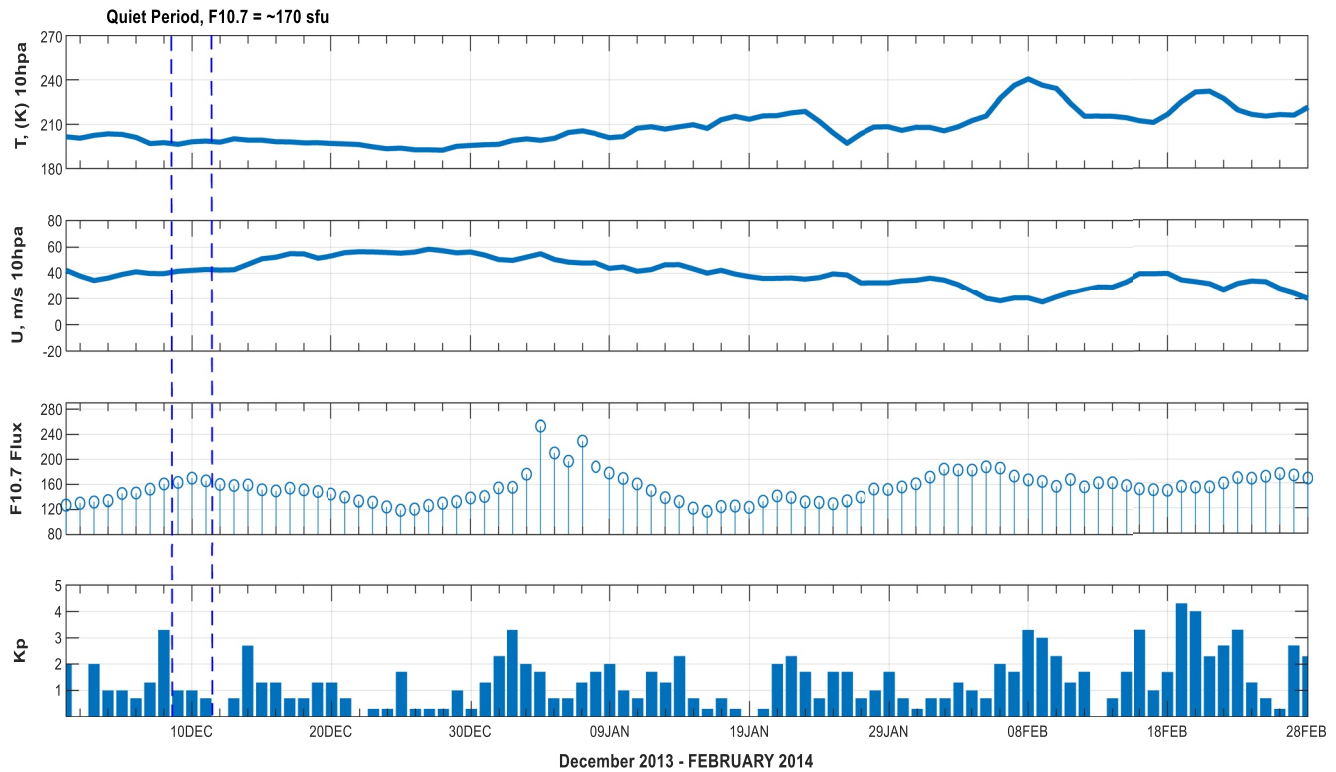
Figure 4. The stratospheric, solar, and geomagnetic parameters during December 2013–February 2014 sudden stratospheric warming events. The two vertical dashed blue lines indicate the period when the solar flux, $F_{10.7}$ = 168.2 sfu (9–11 December 2013).

generally due to the combined effect of thermospheric equatorward wind, thermospheric O/N_2 ratio and the magnetometer inferred upward-directed E X B drift (eastward electric field) and solar flux (photo-ionization). For instance, in the presence of the ongoing photo-ionization, the SSW-induced thermospheric equatorward wind effect (Figure 7a) is primarily responsible for moving the northern EIA crest closer to the magnetic equator on 3–6 January 2013. Then, both the eastward electric field (Figure 8a) and thermospheric composition O/N_2 ratio effects are secondary (weakened, Figure 11). This is similar to De Paula et al. (2015) works as they reported how the SSW-induced thermospheric equatorward wind effect majorly moved the southern crest equatorward during SSW periods. Also, we observed that the combined effect of increasing SSW-induced thermospheric equatorward wind effect and composition O/N_2 is related to the increasing SSW-time down-welling O/N_2 ratio (Figure 11) that is being transported to the low latitude ionosphere on 8 and 12–13 January 2013. This is primarily responsible for transporting the northern EIA crest equatorward as the eastward electric field effect is secondary. The EIA crests seen around 18:00 UT (13:00 LT) on most of the days are higher at the northern crest, LPUC (4.25°N), than the southern crest, IACR (5.58°S). Also distinct is the re-location of the northern crest from LPUC to ESMR (4.25°N to 13.02°N) on 14 January 2013. Also, its further re-location to BOGT (4.25°N to 16.93°N) on 15–19 January 2013. These results were related to the varying amplitude of the daily EEJ strength in Figures 8a and 8b (magnetometer-inferred E X B drift velocity, Anderson & Araujo-Pradere, 2010). Similar results have been presented in the works of Goncharenko et al. (2013) and Siddiqui Tarique et al. (2018).

During the SSW onset (7 January 2013), a daytime counter electrojet (CEJ) depicting a semidiurnal signature (downward in the morning-afternoon and upward in the afternoon-evening period) was seen in Figures 8a and 8c. This contrasts the well-reported semidiurnal upward (late morning) and downward (afternoon) varying equatorial E X B drift velocity signature (Anderson & Araujo-Pradere, 2010; Chau et al., 2009; Fejer et al., 2010; Sridharan et al., 2009) that increased the low latitude TEC and affected the EIA crests (Kelley et al., 2009). Recall that a semidiurnal signature indicates SSW-time semidiurnal tide in the varying equatorial E X B drift velocity (Chau et al., 2009; Fejer et al., 2010). Due to 2-dimensional pictures, such as a morning CEJ (Figures 8a and 8c) that can be related to a morning westward electric field and indicating that the daytime eastward electric field is not active, could not be seen in the works of Goncharenko et al. (2013) and Siddiqui Tarique et al. (2018). Therefore,
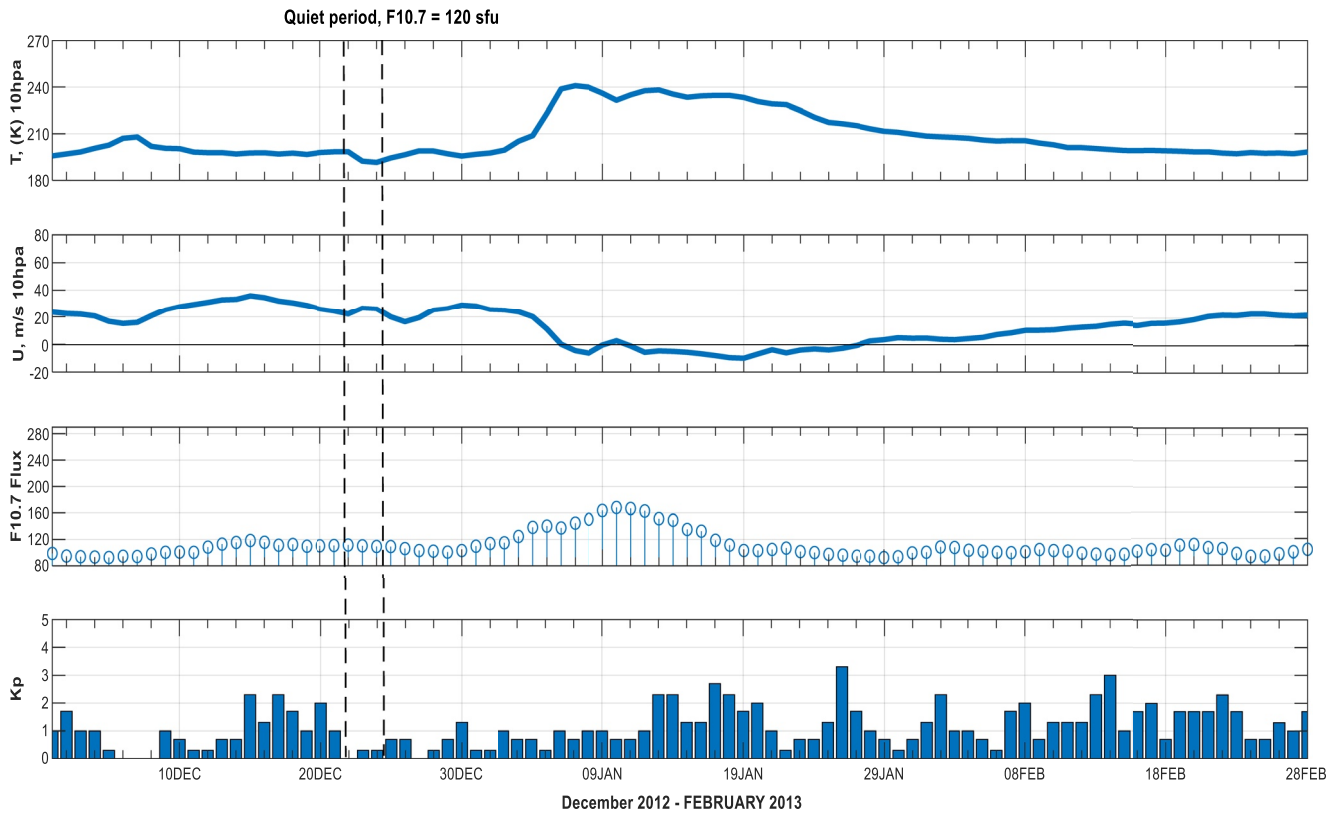
Figure 5. The stratospheric, solar, and geomagnetic parameters during December 2012–February 2013 sudden stratospheric warming events. The two vertical dashed black lines indicate the period when the solar flux, $F_{10.7}$ = 120 sfu (22–24 December 2012).
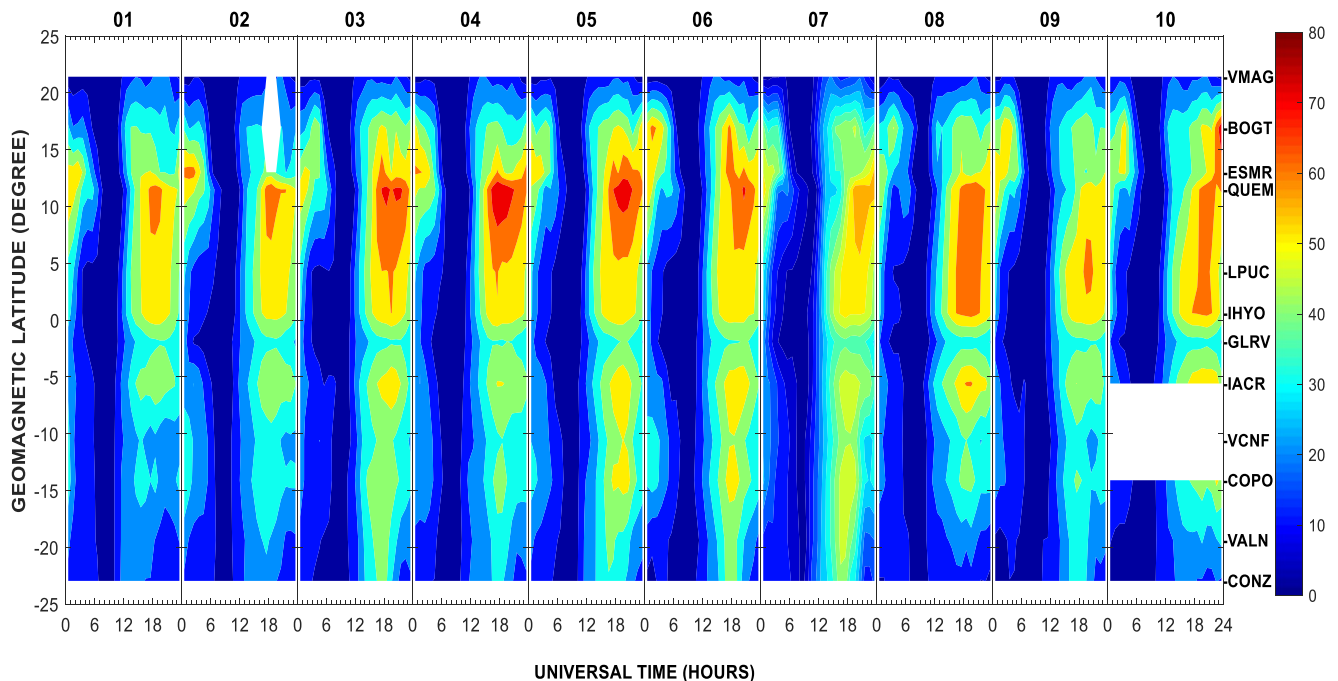

Figure 6. (a) The day-to-day variability of the American equatorial ionization anomaly (EIA) from 01 to 10 December 2012. (b) The day-to-day variability of the American EIA from 11 to 20 December 2012. (c) The day-to-day variability of the American EIA from 21 to 31 December 2012.
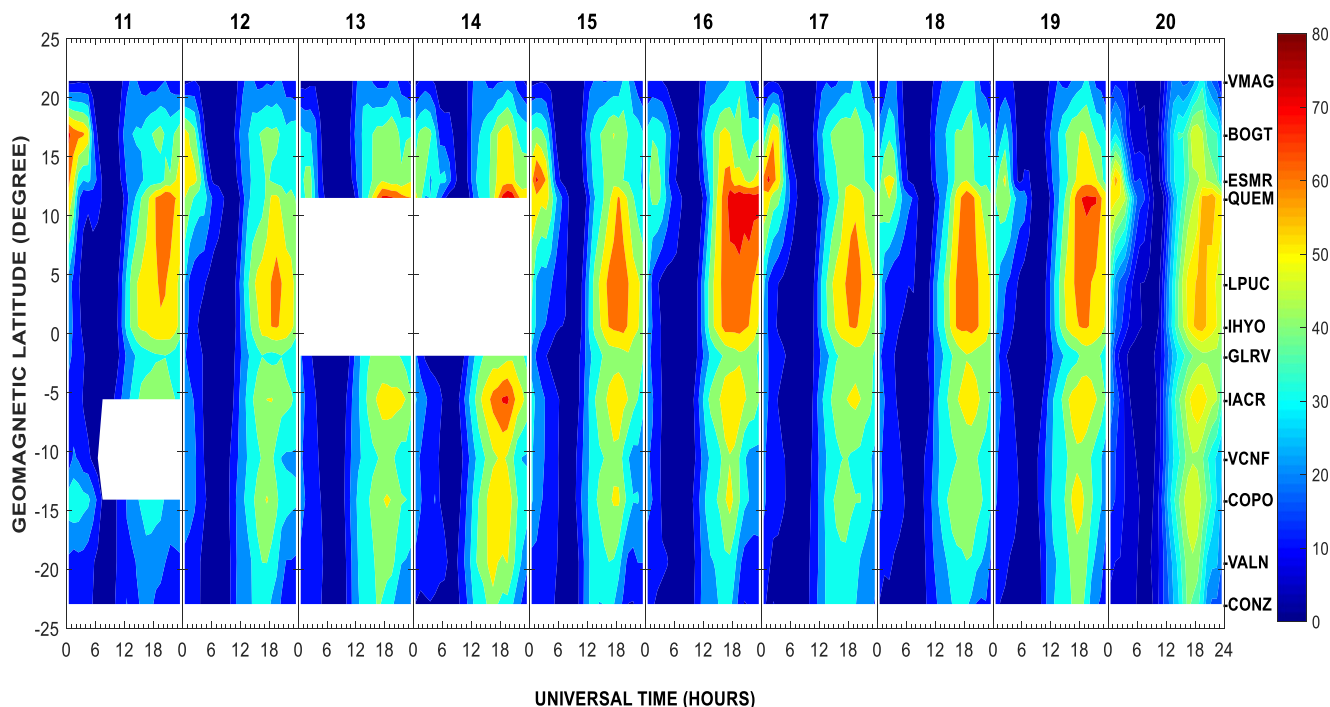
Figure 6. (Continued)

a poleward plasma flow, which the eastward electric field can trigger, is rule-out in this context. To the best of our understanding, simulation and experimental investigations during geomagnetic conditions (Balan et al., 2009; Bolaji et al., 2021) have shown that the daytime westward electric field inhibited EIA formation and supported
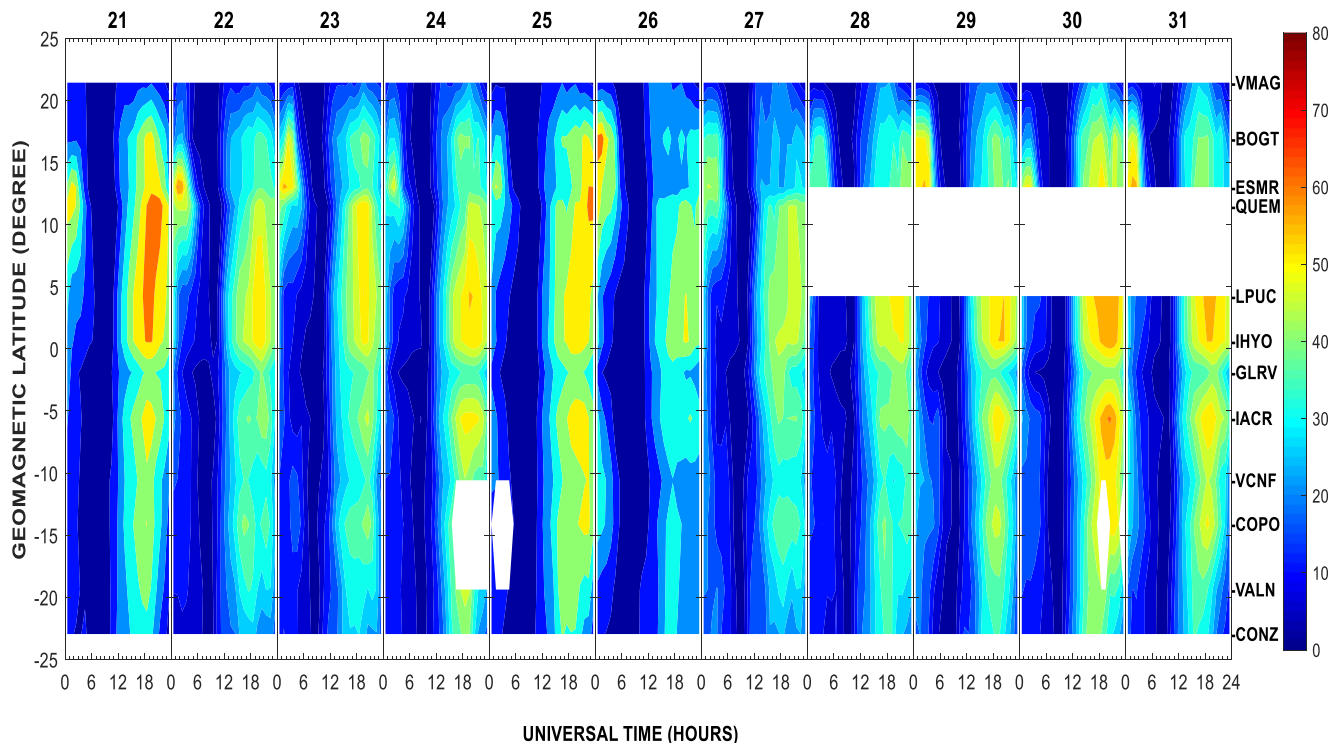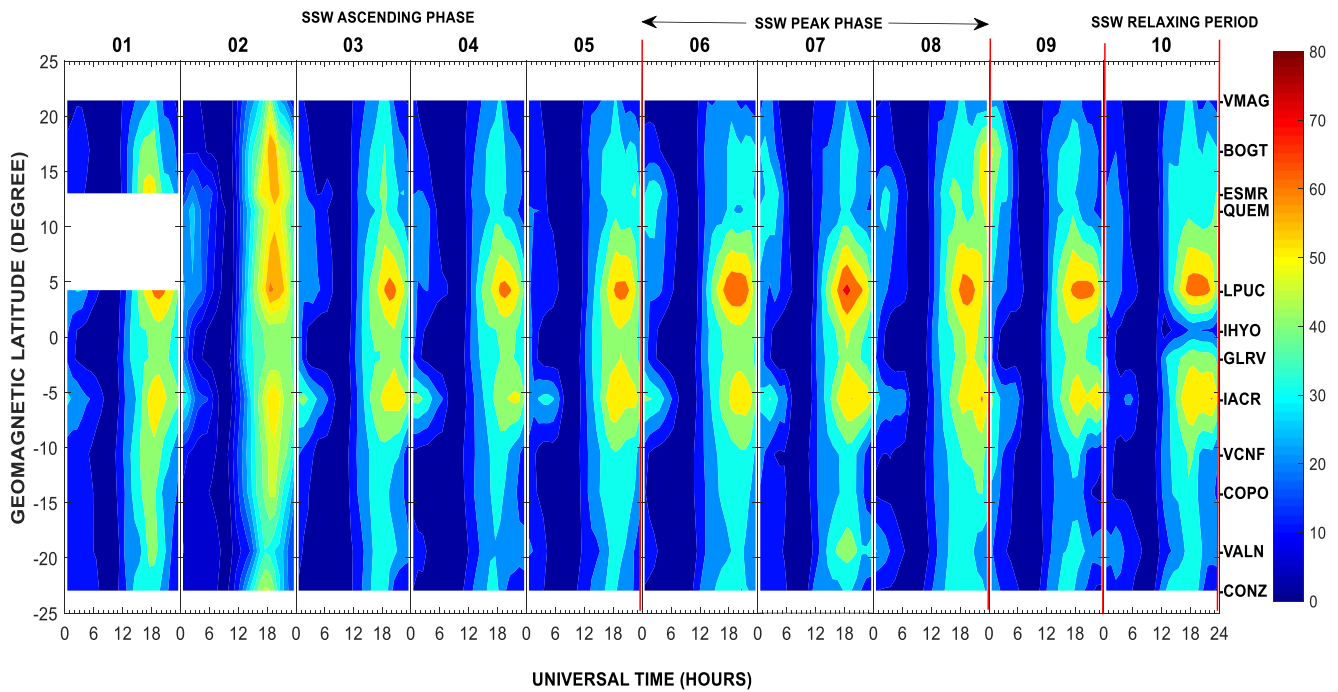

Figure 6. (Continued)

Figure 7. (a) The day-to-day variability of the American equatorial ionization anomaly (EIA) from 01 to 10 January 2013. (b) The day-to-day variability of the American EIA from 11 to 20 January 2013.

the formation of an equatorial peak. Hence, on 7 January 2013, the combined effects of the varying solar flux (photo-ionization production), SSW-time neutral wind and SSW-time thermospheric neutral composition O/ N_2 ratio can be responsible for the EIA formation and its enhancement at the northern (LPUC) compared to the
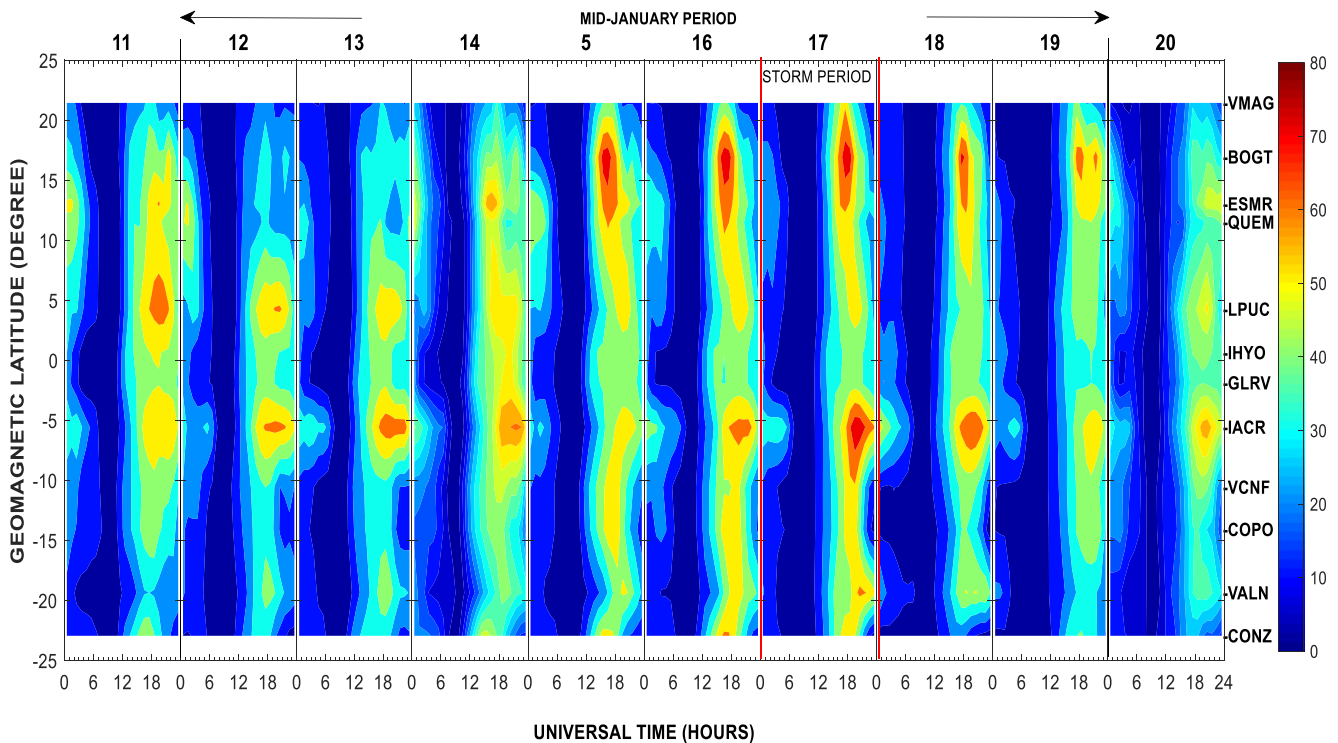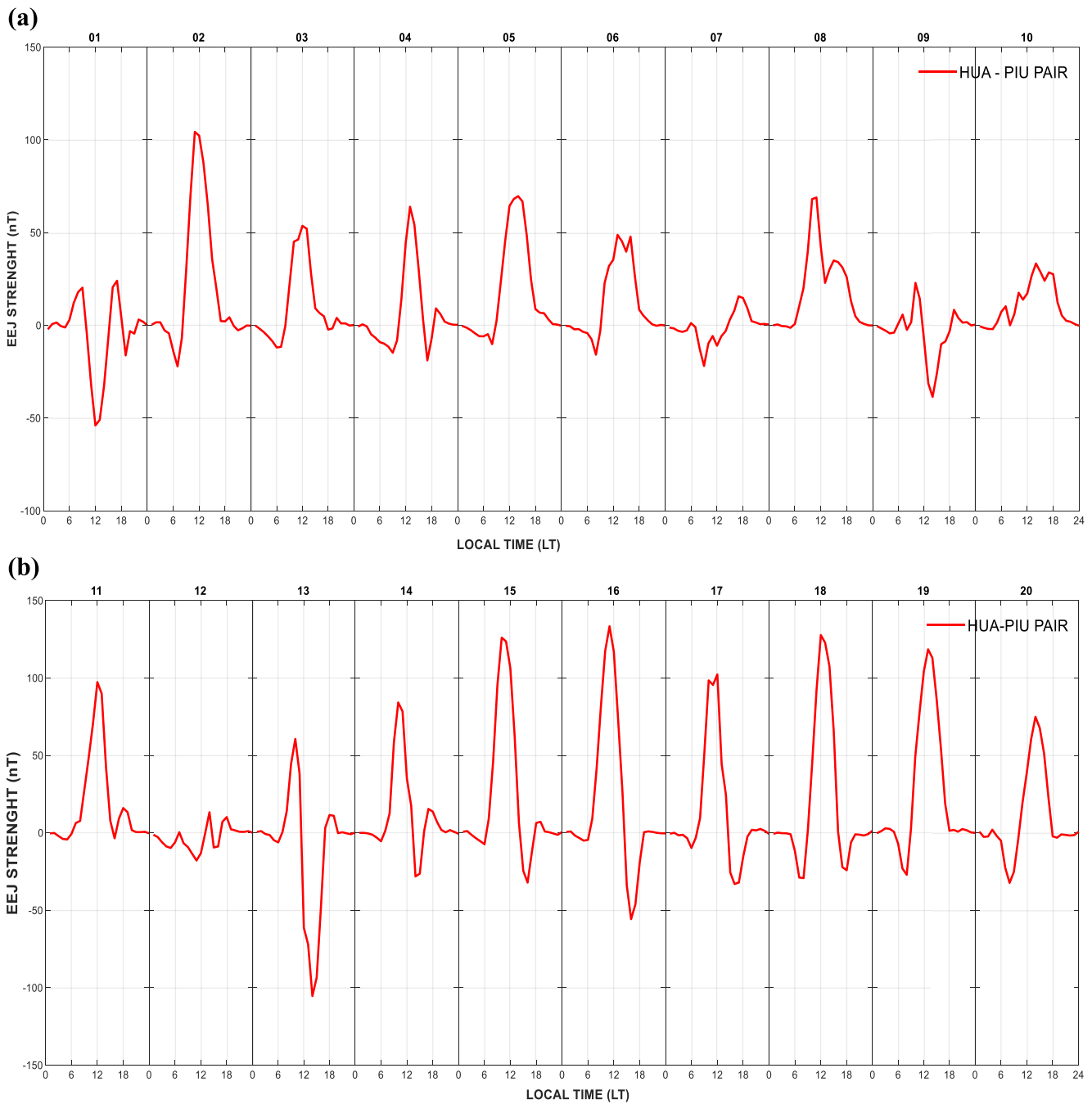

Figure 7. (Continued)

Figure 8. (a and b) The inferred E X B drift over the Northern Hemisphere in the South America during January 2013 sudden stratospheric warming (SSW) events. (c and d) The inferred E X B drift over the Southern Hemisphere in the South America during January 2013 SSW events.

southern (IACR) crest. To clarify this, a major SSW depicted by dramatic changes in the stratospheric temperature (239.9 K, Figure 2a) and zonal mean zonal wind (−5.64 m/s, Figure 2b) at high latitudes on 7 January 2013 triggers the upward propagating waves interacting non-linearly with PW and propagating vertically toward the mesosphere lower thermosphere (MLT) region (Meyer Christian, 1999). This set up an upward and equatorward circulation in the MLT region (Liu & Roble, 2002). Due to the heating of the high latitude thermosphere by the stratospheric temperature, meridional circulation changes associated with the varying SSW modulated the zonal mean zonal wind and connected the MLT with the middle and low latitude ionosphere (Laskar et al., 2014). As the suspected SSW-time equatorward wind due to heating of the thermosphere coupled the ionosphere with

(c)

(d)
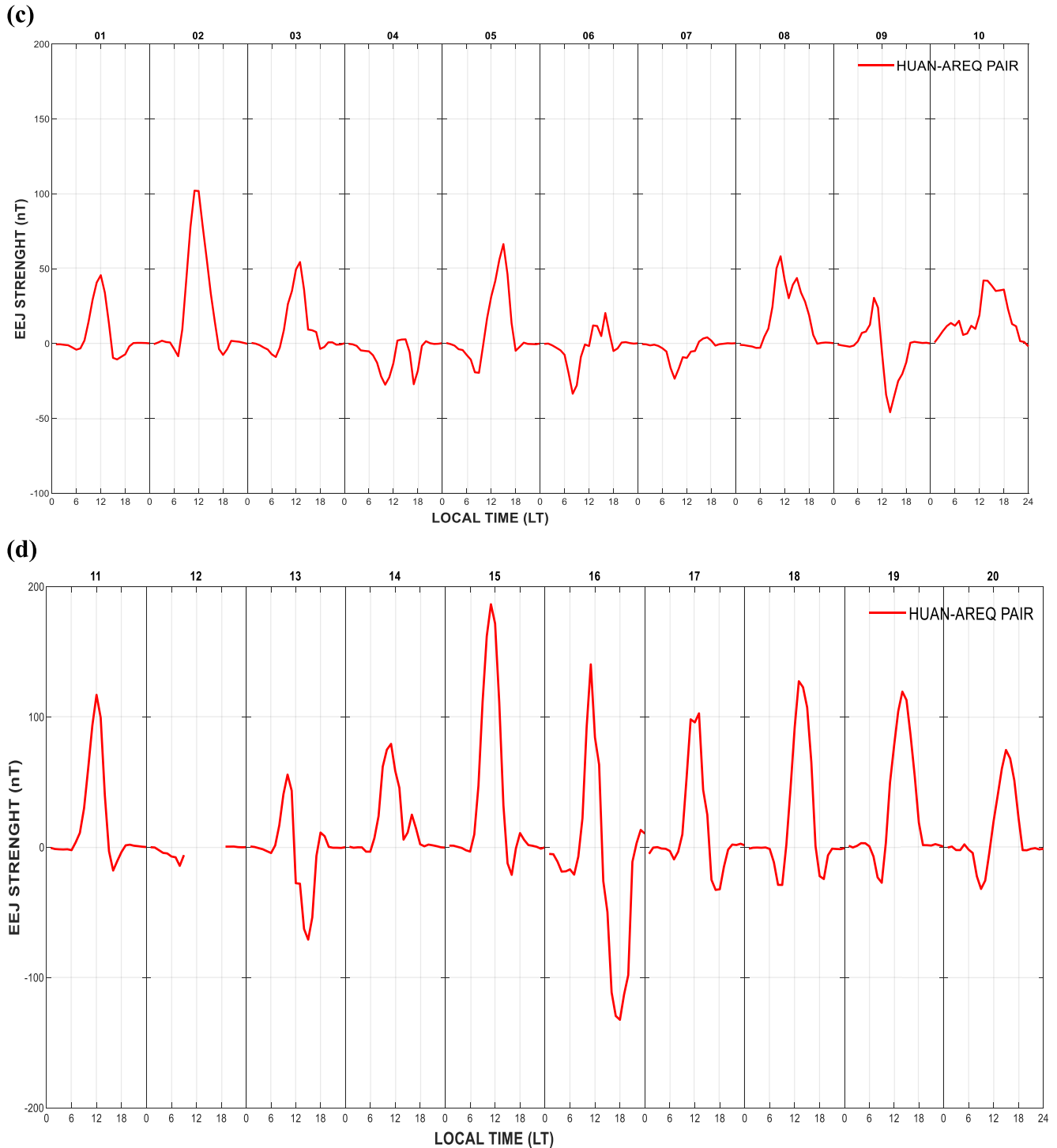
Figure 8. (Continued)

insignificant hindrance from the poleward plasma flow (especially at the middle latitudes), the ionosphere can be raised to higher altitudes of low recombination rate. Obviously, during the SSW-induced day of 7 January 2013, around 75°W, the chemical effect due to the down-welling O/N_2 ratio (Roble et al., 1982) characterized by richer atomic oxygen and poorer molecular nitrogen at the northern high-middle latitudes is slightly higher than that of 6 January 2013 (Figure 11). The SSW-induced equatorward wind can bring along this slightly-high down-welling O/N_2 ratio seen at the northern high-middle latitudes to the low latitude ionosphere on 7 January 2013. Then, the

Figure 9. (a) The daily total electron content (TEC) variations and averaged TEC value (TECquiet) during the periods when the $F_{10.7} = 140$ sfu (2–4 January 2012) in the American sector. (b) The daily TEC variations and averaged TEC value (TECquiet) during the periods when the $F_{10.7} = 166.2$ sfu (9–11 December 2013) in the American secto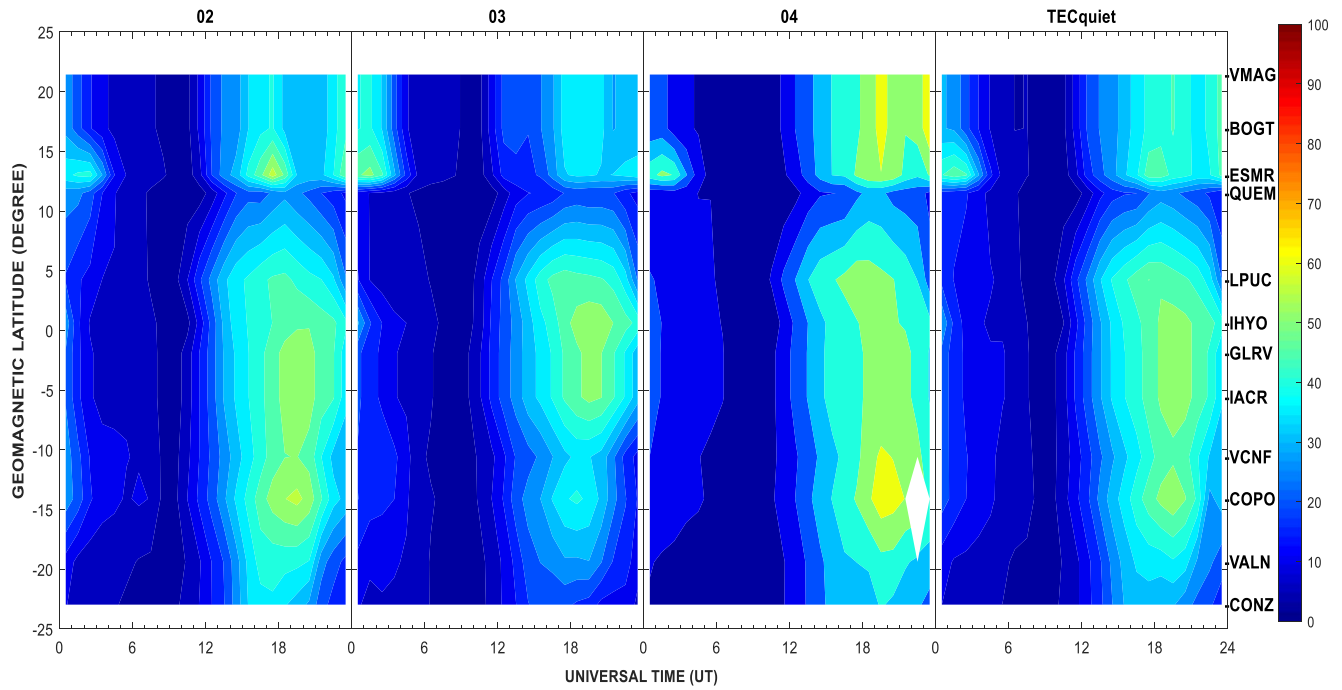r. (c) The daily TEC variations and averaged TEC value (TECquiet) during the periods when the $F_{10.7} = 120$ sfu (22–24 December 2012) in the American sector.
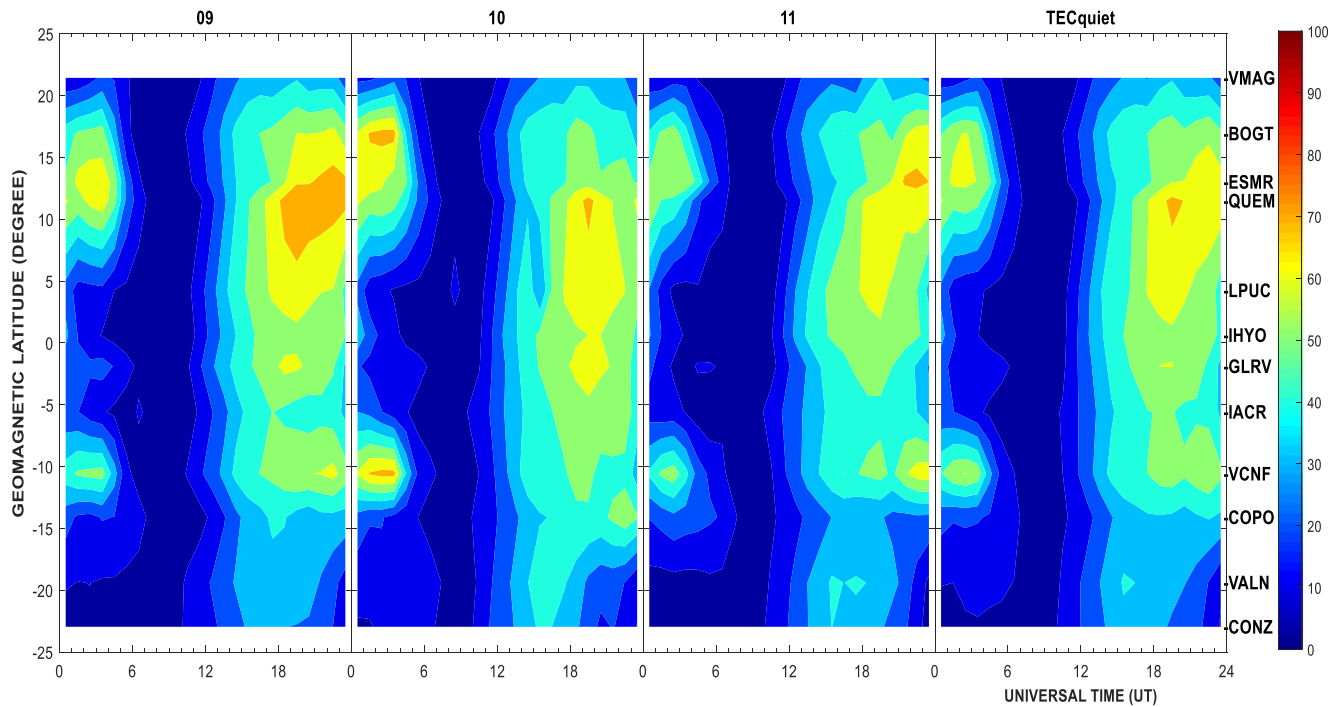

Figure 9. (Continued)
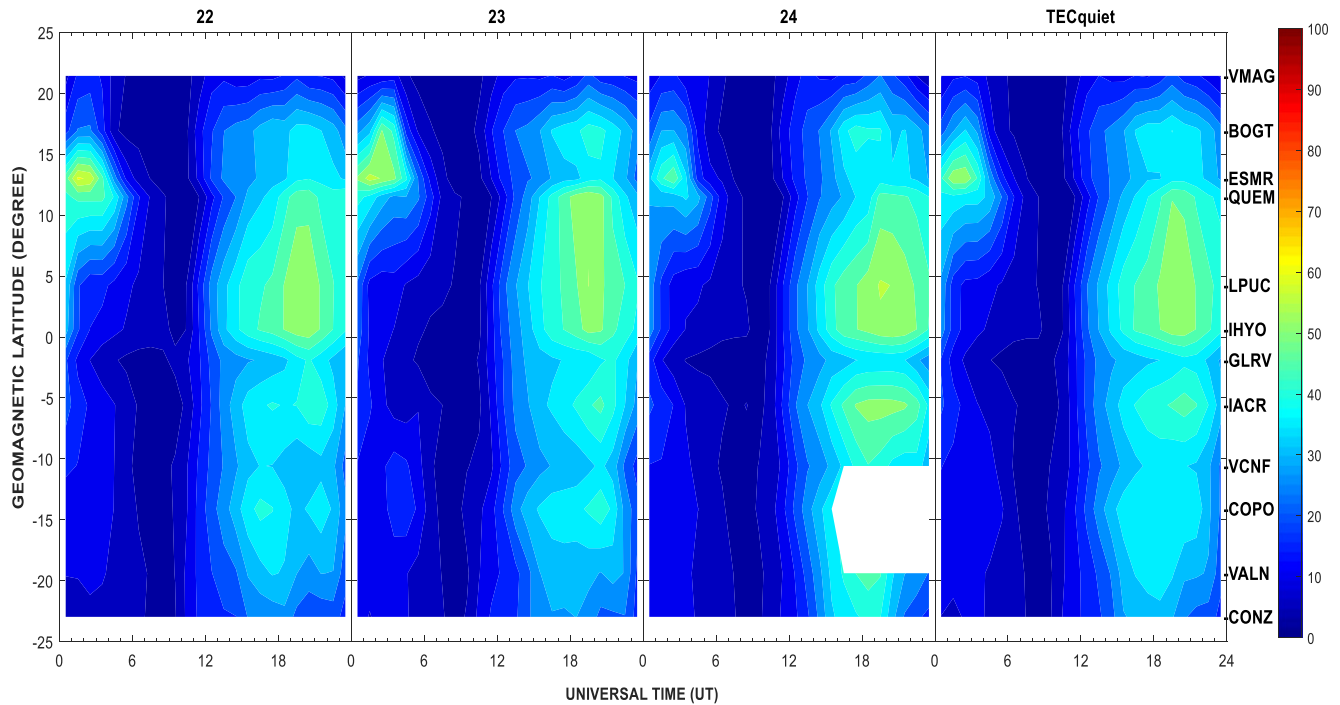
Figure 9. (Continued)
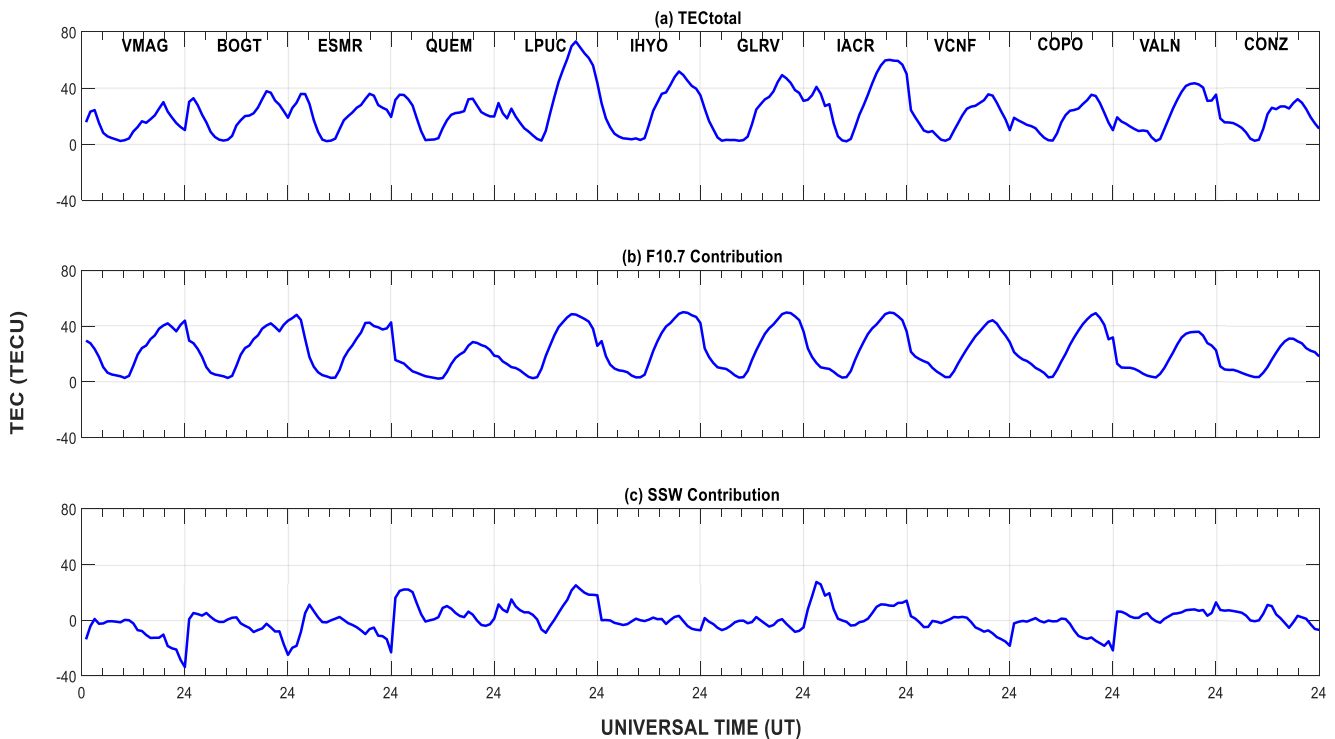
Figure 10. (a) Station by station line plots of the total total electron content (TEC), and individual TEC contributions by the solar flux and sudden stratospheric warming (SSW) to the American low-latitude ionosphere during the 2013 SSW onset (7 January 2013). (b) Station by station line plots of the total total electron content (TEC), and individual TEC contributions by the solar flux and SSW to the American low-latitude ionosphere during the 2013 SSW relaxing phase (10 January 2013). Station by station line plots of the total TEC, and individual TEC contributions by the solar flux and SSW to the American low-latitude ionosphere during the 2013 mid-January (15–16 January 2013). (c) Station by station line plots of the total TEC, and individual TEC contributions by the solar flux and SSW to the American low-latitude ionosphere during the 2013 mid-January (15–16 January 2013). (d) Station by station line plots of the total TEC, and individual TEC contributions by the solar flux, SSW and storm to the American low-latitude ionosphere during the ongoing SSW modulated by minor storm (17 January 2013).
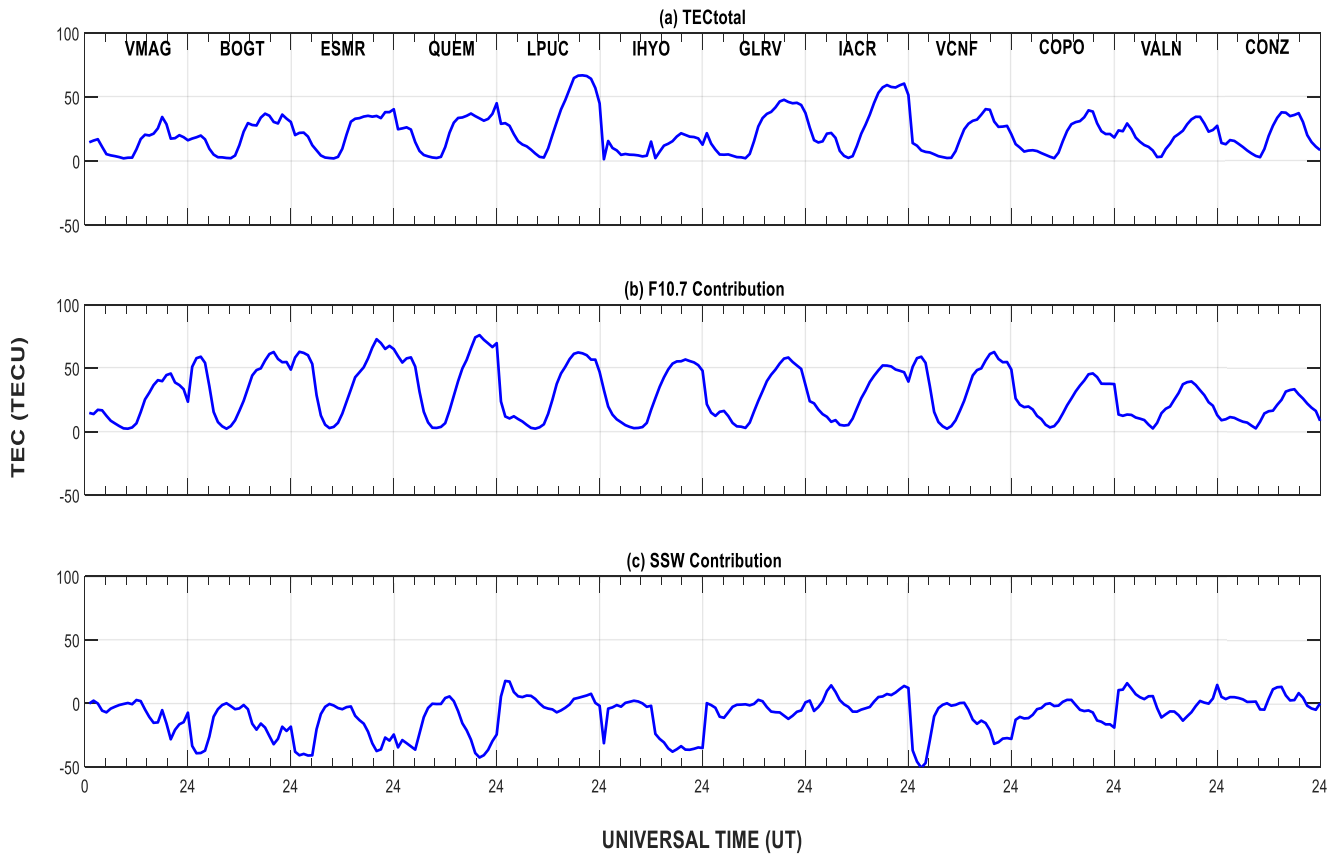
Figure 10. (Continued)

combined effects of the SSW-time equatorward wind, a slight increase in the SSW-time down-welling effect and daytime photo-ionization production can facilitate the well-developed EIA signature and enhance the northern crest more than the southern crest on 7 January 2013. In a similar case on 9 January 2013, there is an increase in the SSW-time down-welling effect (Figure 11). Even though SSW is a northern winter phenomenon where its effect is expected to be dominant, the photo-ionization role was a major one. This was supported by our results in Table 2, revealing that the SSW played a secondary role in facilitating a higher northern crest. For example, solar flux contributed 84% to the northern crest and 85% to the southern crest. In comparison, the SSW effect (SSW-time equatorward wind and down-welling impact) contributed 16% and 15% to the northern and southern crest, respectively. This indicates that SSW contribution to the northern crest was slightly higher than the southern one. These results can be due to the intense competition between the dominating and ongoing photo-ionization versus an unexpected and significant SSW event that is just beginning. This indicates that this initial SSW cannot immediately override the contribution of the ongoing photo-ionization. These factors may be responsible for these relative range values in both hemispheres.

During the major SSW on 10 January, a westerly-directed zonal mean zonal wind flow of 1.6 m/s (Figure 2b) and a conspicuous reduction in the stratospheric temperature (Figure 2a) were observed. This signifies a weak SSW-induced period. In addition to this, is a weak (26 nT) magnetometer-inferred upward E X B drift velocity (Figure 8a) seen around 75°W depicting a weak SSW-time eastward electric field in the ionosphere. Also, the SSW-time down-welling O/N_2 ratio continue to increase at the high latitudes on 10 January 2013 in American sector as the SSW-induced equatorward wind brings it to the low latitude ionosphere. A significant increase in solar flux from 140 sfu (7 January 2013) to 168 sfu (10 January 2013) was obvious in Figure 2. This was also evident in Table 2 on 10 January 2013 as solar flux and SSW effects contributed 90% and 10%, respectively, to the northern crest. Solar flux contributed 77% at the southern crest and SSW contributed 23%. These indicate that during the SSW relaxing phase (10 January 2013), the SSW effect on the ionosphere is not remarkable in the
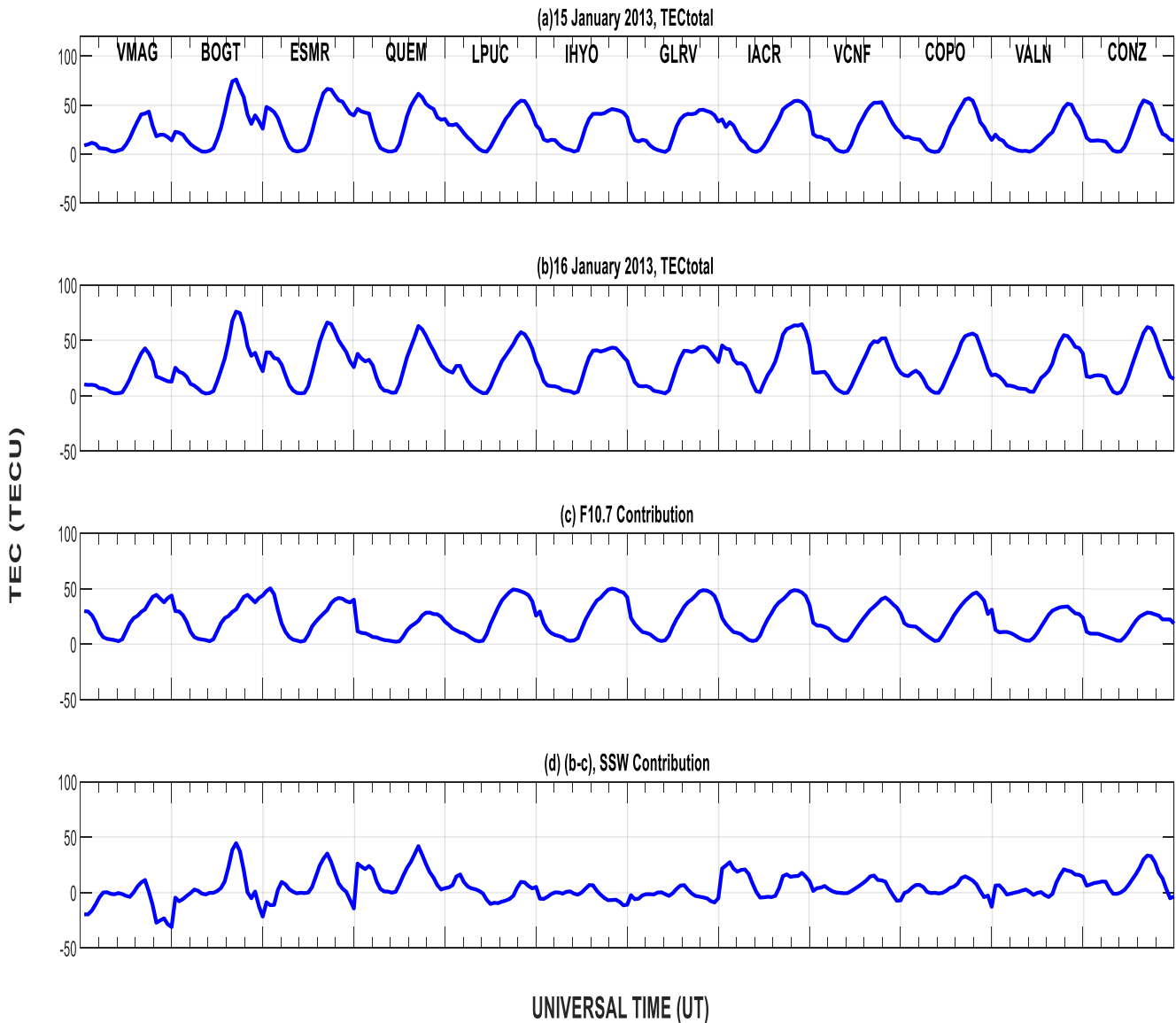
Figure 10. (Continued)

northern winter hemisphere. Therefore, combined effects of the above physical mechanisms can be responsible for the EIA formation with photo-ionization production as the leading factor.

Compared to the SSW onset (7 January 2013), significant re-location of the northern crest from ESMR (14 January 2021) to BOGT station and its TEC enhancement on 15 and 16 January 2013 (mid-January period, Figure 7b) are attributed to intensified SSW conditions (stratospheric temperature, T = 240 K, Figure 2 panel a and zonal mean zonal wind, U = −5.72 m/s − −6.83 m/s, Figure 2b). These intensified SSW conditions modulate the varying semidiurnal inferred E X B drift velocity on 14 January 2013 and significantly increase its value in the morning and CEJ in the afternoon on 15–16 January 2013 (Figure 7b). As mentioned, a similar semidiurnal signature in the inferred E X B drift velocity (Chau et al., 2009; Fejer et al., 2010; Sridharan et al., 2009) increased the low latitude TEC and EIA crests (Kelley et al., 2009). This indicates a large increase in the daytime eastward electric field that transports more ionosphere plasma from around the magnetic equator through the magnetic field lines to higher altitudes. After losing momentum, due to gravity and electron density gradient, this large poleward ionosphere plasma flowing on both sides of the dip equator get deposited at higher latitudes.
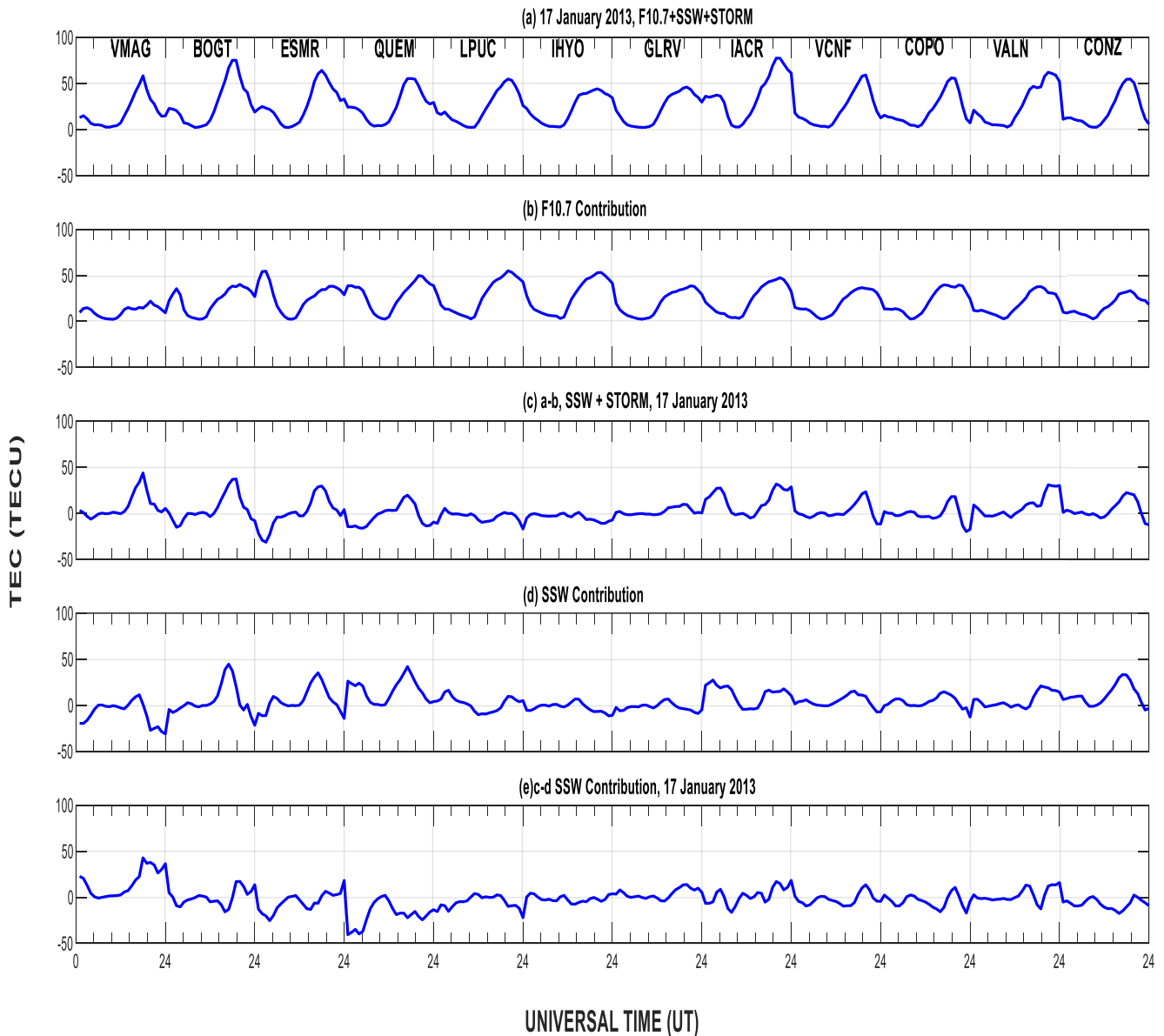
Figure 10. (Continued)

In addition to this is the increase of thermospheric neutral composition O/N_2 ratio (Figure 11) from 0.5 (14 January 2013) to 0.7 (15–16 January 2013). As the SSW-time equatorward wind was transporting the down-welling O/N_2 ratio into the low latitudes, it could not reduce the ongoing stronger poleward plasma flow in the northern hemisphere. Hence, the relocation of the northern crest from ESMR to BOGT while the southern crest location is not changing (Figure 7b). We confirmed that the disparity in the hemispheric crests is due to the SSW, which is a northern winter event, compared to the southern, which is not affected by the SSW event. The combined effect of SSW-time equatorward wind, indirect down-welling O/N_2 and stronger eastward electric field in the northern hemisphere contributed 58% (Table 2) to the increase in TEC magnitude at the northern crest and its relocation. Together with the ongoing daytime production of ionization that contributed 42%, they are responsible for these significant changes seen in EIA signatures on 15–16 January 2013. However, in the southern hemisphere, where the SSW effect rarely modulates the ionosphere, photo-ionization contribution was more prominent (72%) than SSW, which contributed 28%.

Table 2
Showing the Individual Contribution of F10.7, Sudden Stratospheric Warming, and Geomagnetic Storm During the Major and Minor Warmings

07/01/2013	F10.7 (%)	SSW contribution (%)	Storm contribution (%)
Northern Hemisphere	84	16	NIL
Southern Hemisphere	85	15	NIL
10/01/2013			
Northern Hemisphere	90	10	NIL
Southern Hemisphere	77	23	NIL
15-16/01/2013			
Northern Hemisphere	42	58	NIL
Southern Hemisphere	72	28	NIL
17/01/2013			
Northern Hemisphere	51	50	−1
Southern Hemisphere	58	20	22

On 17 January 2013, our results (Figures 7b, 8b and 8d, and day 17 in Figure 11) revealed that the effect of the ongoing intense SSW got modulated by a minor geomagnetic storm (SYM-H of–58 nT), storm-time induced SSW. Contrasting Pedatella et al. (2008)'s work, the ongoing SSW event altered by a minor geomagnetic storm on 17 January 2013 did not disrupt the SSW-induced EIA. The effect of the minor geomagnetic storm of 17 January 2013 during the ongoing major SSW is exciting. It is evident in Figures 8b and 8d as the inferred upward-directed E X B drift at both hemispheres is reduced compared to the SSW-induced days (15, 16, 18 and 19 January 2013). Also, as shown in Table 2 on 17 January 2013, the minor geomagnetic storm influence reduced SSW contributions at the northern crest to 50% and increased the photo-ionization contribution to 51%. Therefore, the minor geomagnetic storm's overall contribution to the northern crest at the expense of the combined lead role of SSW and photo-ionization was −1%. The reduction in SSW contribution can be related to reduce inferred upward-directed E X B drift, partly responsible for the slight decrease in the northern crest. Recall that during the 2013 SSW event, Maute et al. (2015) reported that the wind dynamo, which can modulate the daytime vertical drift, was attributed to the migrating solar and semidiurnal westward propagating tides. At the southern crest, the minor geomagnetic storm effect reduces both the photo-ionization (58%) and SSW (20%) contributions compared to 15–16 January 2013 (Table 2). Then, the minor geomagnetic storm contributed 22% at the southern crest. Overall, the minor geomagnetic storm and the SSW play a secondary role in contributing to the southern crest as photo-ionization leads. Since photo-ionization is leading and SSW contributed the least, direct ionization contribution to the southern crest overrides the varying daytime vertical drift and the PPEF that can be facilitated by the SSW effect and minor geomagnetic storm on 17 January 2013, respectively.

Our results agree with the work of Ribeiro et al. (2019) on the higher southern crest of 17 January 2013 (77 TECU) compared to 16 January 2013 (65 TECU). However, their suggestion of invoking traveling ionospheric disturbances, TIDs cannot be substantiated as the varying TEC residual wave-form reported in their work is actually of SSW origin, as shown by our efforts in this work (Figures 10d and 10e). Also, our results strongly disagree with the suggestion of Goncharenko et al. (2013) that a brief minor geomagnetic activity of 17 January 2013 will not drive these above-described variations in the low latitude TEC. Our observed results strongly agree with the suggestions of Maute et al. (2015), Hagan et al., 2015, Pedatella et al. (2016) and Pedatella and Liu (2018) in that combined effect of the lower atmospheric forcing and a geomagnetic storm is important to specifying and forecasting the near-Earth space environment.

4. Conclusions

In this paper, we have presented and discussed the response of the ionospheric TEC to 2013 SSW event and associated geomagnetic storm over the American low latitudinal sector. The main results from the study are as follow:
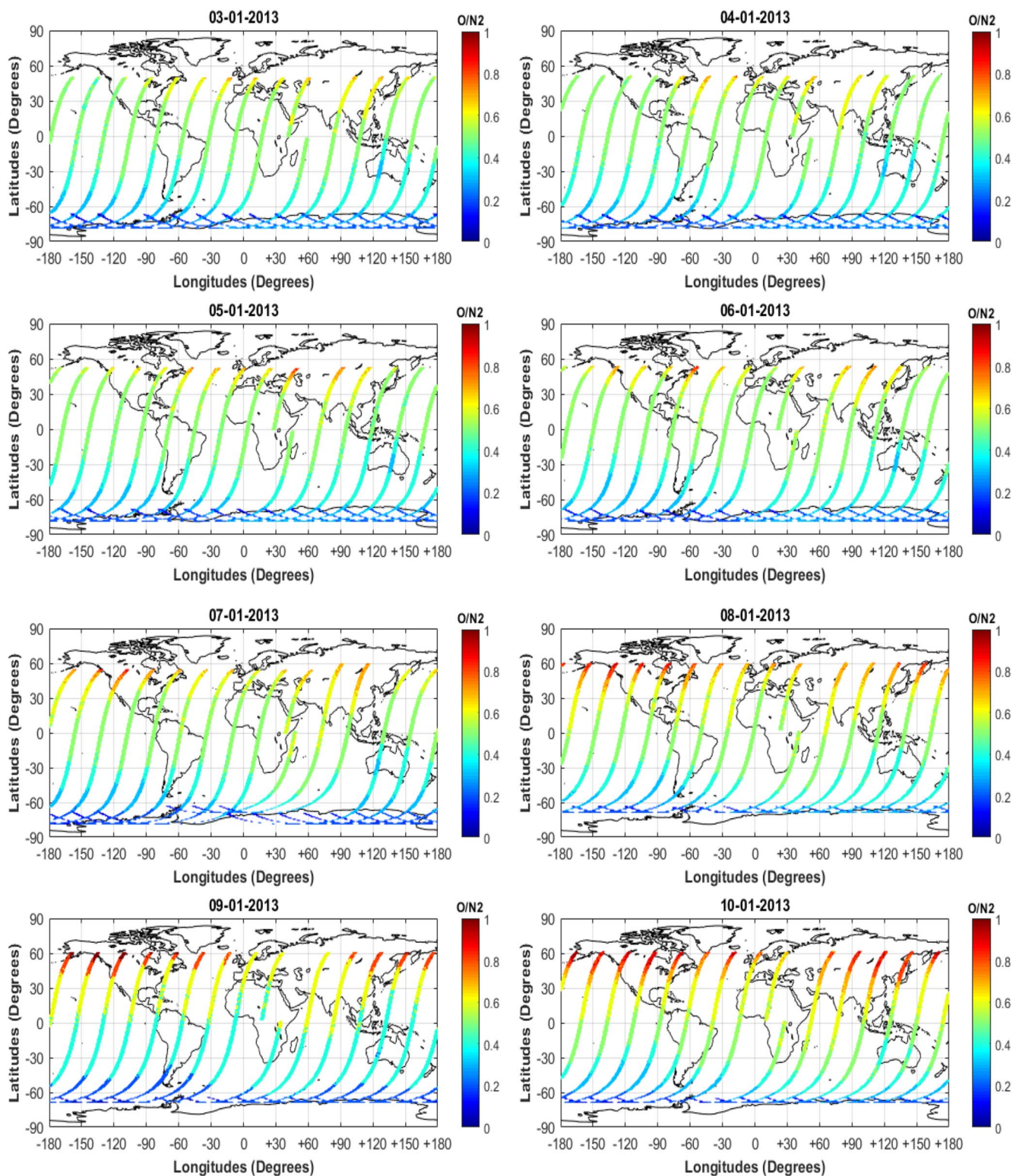
Figure 11. Thermospheric O/N$_2$ ratio from GUVI for the period of 03–20 January 2013.
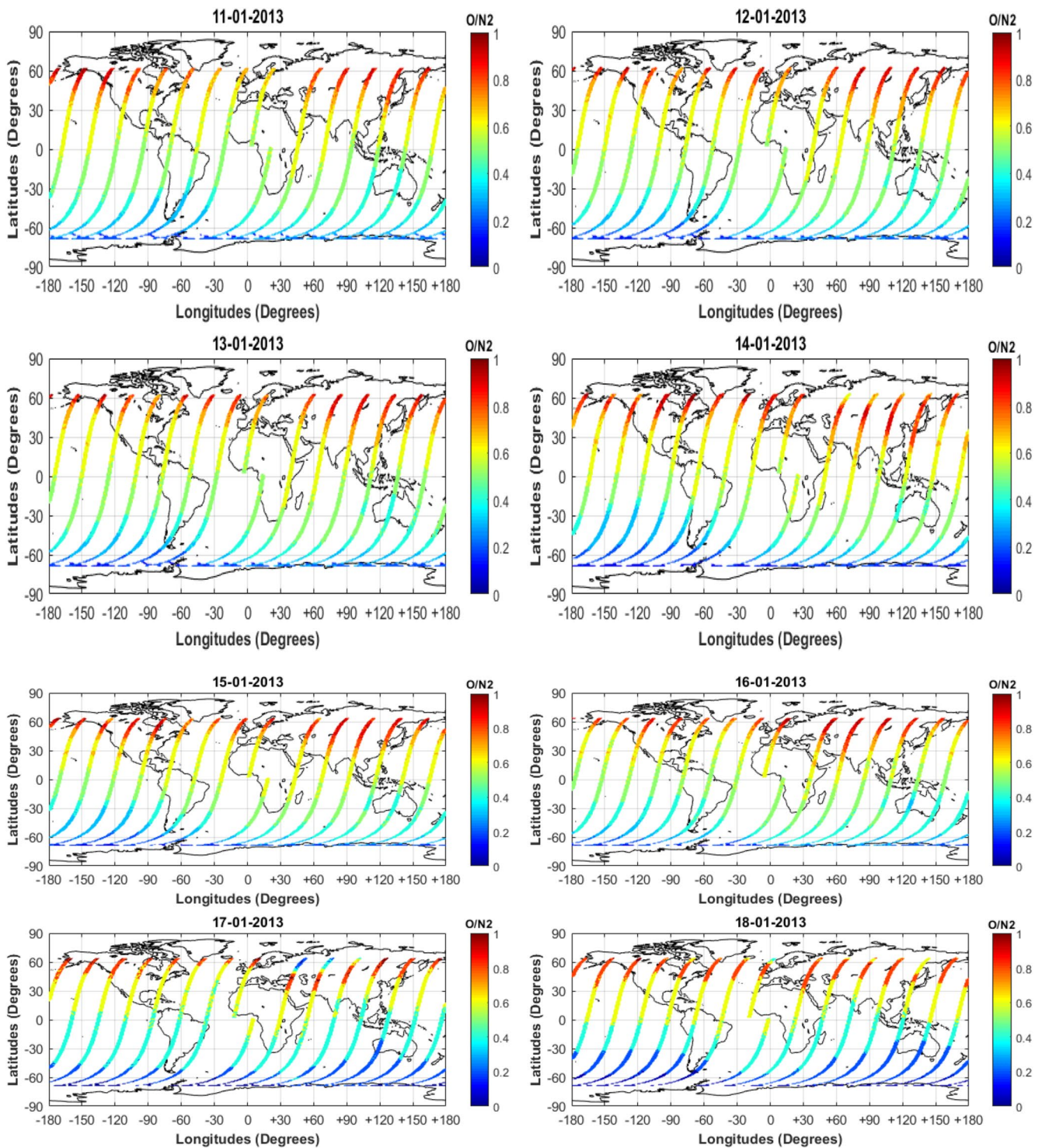
Figure 11. (Continued)

1. The late morning inferred downward-directed E X B drift was inactive in forming the EIA signature during the SSW onset. In contrast, significant enhancement in the varying inferred upward-directed E X B drift was observed during the mid-January at both hemispheres

2. With or without the inferred E X B drift, a well-developed EIA signature during SSW events is due to the combined effects of an increase in SSW-time equatorward wind, SSW-time down-welling O/N_2 effect and daytime photo-ionization production

3. The SSW (solar flux) effect during the SSW onset contributed 16% (84%) and 15% (85%) to the northern and southern crests, respectively. The closest values may be due to intense competition between the ongoing photo-ionization and significant SSW events

4. During the SSW relaxing phase, a westerly-directed zonal mean zonal wind and a slight reduction in the stratospheric temperature, indicating a weak SSW period, is responsible for the reduced magnetometer-inferred upward-directed E X B drift

5. Compared to the SSW onset period, significant re-location of the northern crests during the mid-January is attributed to the intensified SSW condition that modulated the varying semidiurnal inferred E X B drift

6. At the expense of the combined role of SSW photo-ionization, the minor geomagnetic storm effect contributed −1% to the northern crest. The reduction in SSW contribution can be related to reduce inferred upward-directed E X B drift

7. At the southern crest, the minor geomagnetic storm contributed 22% by reducing photo-ionization (58%) and SSW (20%) contributions. Notwithstanding, the enhancement in TEC magnitude resulted from direct ionization, as a leading factor that overrides the varying daytime vertical drift and the PPEF that can be facilitated by the SSW effect and minor geomagnetic storm on 17 January 2013, respectively

8. Contrary to the assertion of Pedatella et al. (2008) that investigated July 2004 events, the interplay between the ongoing major SSW and a geomagnetic storm of 17 January 2013 did not disrupt the EIA signature

9. Our observation agrees with the intensification of ionospheric plasma seen at the southern crest, as seen in the work of Ribeiro et al. (2019). However, we confirm that the event was originally driven by an SSW and contrasted Ribeiro et al. (2019) suggestions that it originated from gravity waves drove it. A major SSW was ongoing before being overlapped by a brief and minor geomagnetic storm

10. Contrary to Goncharenko et al. (2013) suggestion, we found that geomagnetic activity, among others, is a factor to reckon with concerning driving the ionospheric variations seen on 17 January 2013. Hence, modelers should consider SSW forcing along geomagnetic storm forcing in their future modeling efforts. This would improve the forecasting of the near-Earth space environment

Finally, we concluded that it is now becoming increasingly clear that understanding the forcing from SSW is critically important for the space weather modeling community to predict and forecast the day-to-day TEC during the northern wintertime in the low latitude. Thus, incorporating the forcing due to SSW during the northern wintertime into the future modeling efforts is critically important to accurately characterize the day-to-day variability of TEC in the low latitude ionosphere.

Data Availability Statement

The stratospheric, geomagnetic and solar activity data used in this study were retrieved from the websites of the NOAA Physical Sciences Laboratory (https://psl.noaa.gov), NASA OMNIweb service, https://omniweb.gsfc.nasa.gov/, and the National Oceanic and Atmospheric Administration (NOAA), solar data service at https://www.ngdc.noaa.gov/stp/solar/solardataservices.html respectively. The total electron content (TEC) data from the Global Positioning System (GPS) receivers are freely available online via National Aeronautics and Space Administration (NASA) Archive of Space Geodesy Data (cddis.nasa.gov/archive/gnss/data/) and SONEL (www.sonel.org). The magnetometer data were downloaded from the International Real-time Magnetic Observatory Network, INTERMAGNET (www.intermagnet.org), and the Low Ionospheric Sensor Network (LISN) magnetometers (http://lisn.igp.gob.pe/data/) operated by the Instituto Geofisico del Peru (IGP). The thermospheric O/N_2 column density data is optically obtained from NASA Thermosphere Ionosphere Mesosphere Energetics and Dynamics satellite (TIMED/GUVI) Far Ultraviolet (FUV) airglow instruments at http://guvitimed.jhuapl.edu.

References

Anderson, D., & Araujo-Pradere, E. A. (2010). Sudden stratospheric warming event signatures in daytime E x B drift velocities in the Peruvian and Philippine longitude sectors for January 2003 and 2004. *Journal of Geophysical Research*, *115*(8), 1–7. https://doi.org/10.1029/2010JA015337

Balan, N., & Bailey, G. J. (1995). Equatorial plasma fountain and its effects: Possibility of an additional layer. *Journal of Geophysical Research*, *100*(A11), 21421–21432. https://doi.org/10.1029/95JA01555

Balan, N., Batista, I. S., Abdu, M. A., MacDougall, J., & Bailey, G. J. (1998). Physical mechanism and statistics of occurrence of an additional layer in the equatorial ionosphere. *Journal of Geophysical Research*, *103*(A12), 29169–29181. https://doi.org/10.1029/98JA02823

Balan, N., Shiokawa, K., Otsuka, Y., Watanabe, S., & Bailey, G. J. (2009). Super plasma fountain and equatorial ionization anomaly during penetration electric field. *Journal of Geophysical Research*, *114*(A3), A03310. https://doi.org/10.1029/2008JA013768

Balan, N., Souza, J., & Bailey, G. J. (2018). Recent developments in the understanding of equatorial ionization anomaly: A review. *Journal of Atmospheric and Solar-Terrestrial Physics*, *171*, 3–11. https://doi.org/10.1016/j.jastp.2017.06.020

Blanc, M., & Richmond, A. D. (1980). The ionospheric disturbance dynamo. *Journal of Geophysical Research*, *85*(A4), 1669–1686. https://doi.org/10.1029/ja085ia04p01669

Bolaji, O., Owolabi, O., Falayi, E., Jimoh, E., Kotoye, A., Odeyemi, O., et al. (2017). Observations of equatorial ionization anomaly over Africa and Middle East during a year of deep minimum. *Annales Geophysicae*, *35*(1), 123–132. https://doi.org/10.5194/angeo-35-123-2017

Bolaji, O. S., Adeniyi, J. O., Radicella, S. M., & Doherty, P. H. (2012). Variability of total electron content over an equatorial West African station during low solar activity. *Radio Science*, *47*(1), RS1001. https://doi.org/10.1029/2011RS004812

Bolaji, O. S., Fashae, J. B., Adebiyi, S. J., Owolabi, C., Adebesin, B. O., Kaka, R. O., et al. (2021). Storm time effects on latitudinal distribution of ionospheric TEC in the American and Asian-Australian sectors: August 25–26, 2018 geomagnetic storm. *Journal of Geophysical Research: Space Physics*, *126*, e2020JA029068. https://doi.org/10.1029/2020JA029068

Bolaji, O. S., Owolabi, O. P., Falayi, E., Yamazaki, Y., Jimoh, E., Rabiu, A. B., et al. (2016). Solar quiet current response in the African sector due to a 2009 sudden stratospheric warming event. *Journal of Geophysical Research: Space Physics*, *121*(8), 8055–8065. https://doi.org/10.1002/2016JA022857

Bolaji, O. S., Oyeyemi, E. O., Jimoh, O. E., Fujimoyo, A., Doherty, P. H., Owolabi, O. P., et al. (2019). Morphology of the equatorial ionization anomaly in Africa and Middle East due to a sudden stratospheric warming event. *Journal of Atmospheric and Solar-Terrestrial Physics*, *184*, 37–56. https://doi.org/10.1016/j.jastp.2019.01.006

Chau, J. L., Aponte, N. A., Cabassa, E., Sulzer, M. P., Goncharenko, L. P., & Gonzlez, S. A. (2010). Quiet time ionospheric variability over Arecibo during sudden stratospheric warming events. *Journal of Geophysical Research*, *115*(9), 2–9. https://doi.org/10.1029/2010JA015378

Chau, J. L., Fejer, B. G., & Goncharenko, L. P. (2009). Quiet variability of equatorial E × B drifts during a sudden stratospheric warming event. *Geophysical Research Letters*, *36*(5), 1–4. https://doi.org/10.1029/2008GL036785

De Jesus, R., Batista, I. S., Jonah, O. F., de Abreu, A. J., Fagundes, P. R., Venkatesh, K., & Denardini, C. M. (2017). An investigation of the ionospheric disturbances due to the 2014 sudden stratospheric warming events over Brazilian sector. *Journal of Geophysical Research: Space Physics*, *122*(11), 11698–11715. https://doi.org/10.1002/2017ja024560

De Paula, E. R., Jonah, O. F., Moraes, A. O., Kherani, E. A., Fejer, B. G., Abdu, M. A., et al. (2015). Low-latitude scintillation weakening during sudden stratospheric warming events. *Journal of Geophysical Research: Space Physics*, *120*(3), 2212–2221. https://doi.org/10.1002/2014JA020731

Fagundes, P. R., Cardoso, F. A., Fejer, B. G., Venkatesh, K., Ribeiro, B. A. G., & Pillat, V. G. (2016). Positive and negative GPS-TEC ionospheric storm effects during the extreme space weather event of March 2015 over the Brazilian sector. *Journal of Geophysical Research: Space Physics*, *121*(6), 5613–5625. https://doi.org/10.1029/2015JA022214

Fejer, B. G., Olson, M. E., Chau, J. L., Stolle, C., Lühr, H., Goncharenko, L. P., et al. (2010). Lunar-dependent equatorial ionospheric electrodynamic effects during sudden stratospheric warmings. *Journal of Geophysical Research*, *115*(8), 1–9. https://doi.org/10.1029/2010JA015273

Fejer, B. G., Tracy, B. D., Olson, M. E., & Chau, J. L. (2011). Enhanced lunar semidiurnal equatorial vertical plasma drifts during sudden stratospheric warmings. *Geophysical Research Letters*, *38*(21), 2–6. https://doi.org/10.1029/2011GL049788

Forbes, J. M. (2000). Wave coupling between the lower and upper atmosphere: Case study of an ultra-fast Kelvin wave. *Journal of Atmospheric and Solar-Terrestrial Physics*, *62*, 1603–1622.

Fuller-Rowell, T. J., Codrescu, M. V., Moffett, R. J., & Quegan, S. (1994). Response of the thermosphere and ionosphere to geomagnetic storms. *Journal of Geophysical Research*, *99*(A3), 3893. https://doi.org/10.1029/93JA02015

Fuller-Rowell, T. J., Codrescu, M. V., Rishbeth, H., Moffett, R. J., & Quegan, S. (1996). On the seasonal response of the thermosphere and ionosphere to geomagnetic storms. *Journal of Geophysical Research*, *101*(A2), 2343–2353. https://doi.org/10.1029/95JA01614

Goncharenko, L., Chau, J. L., Condor, P., Coster, A., & Benkevitch, L. (2013). Ionospheric effects of sudden stratospheric warming during moderate-to-high solar activity: Case study of January 2013. *Geophysical Research Letters*, *40*(19), 4982–4986. https://doi.org/10.1002/grl.50980

Goncharenko, L. P., Chau, J. L., Liu, H.-L., & Coster, A. J. (2010). Unexpected connections between stratosphere and ionosphere. *Geophysical Research Letters*, *37*(10), L10101. https://doi.org/10.1029/2010GRL043125

Goncharenko, L. P., Coster, A. J., Chau, J. L., & Valladares, C. E. (2010). Impact of sudden stratospheric warming on equatorial ionization anomaly. *Journal of Geophysical Research*, *115*(A10), A00G07. https://doi.org/10.1029/2010JA015400

Gonzales, C. A., Kelley, M. C., Fejer, B. G., Vickrey, J. F., & Woodman, R. F. (1979). Equatorial electric fields during magnetically disturbed conditions: 2. Implications of simultaneous auroral and equatorial measurements. *Journal of Geophysical Research*, *84*(A10), 5803–5812. https://doi.org/10.1029/JA084iA10p05803

Hagan, M. E., Häusler, K., Lu, G., Forbes, J. M., & Zhang, X. (2015). Upper thermospheric responses to forcing from above and below during 1–10 April 2010: Results from an ensemble of numerical simulations. *Journal of Geophysical Research: Space Physics*, *120*(4), 3160–3174. https://doi.org/10.1002/2014JA020706

Hanson, W. B., & Moffet, R. J. (1966). Ionization transport effects in the equatorial F region. *Journal of Geophysical Research*, *71*(23), 5559–5572. https://doi.org/10.1029/jz071i023p05559

Jonah, O. F., De Paula, E. R., Kherani, E. A., Dutra, S. L. G., & Paes, R. R. (2014). Atmospheric and ionospheric response to sudden stratospheric warming of January 2013. *Journal of Geophysical Research: Space Physics*, *119*(6), 4973–4980. https://doi.org/10.1002/2013JA019491

Kalnay, E., Kanamitsu, M., Kistler, R., Collins, W., Deaven, D., Gandin, L., et al. (1996). The NCEP/NCAR 40-year reanalysis project. *Bulletin of the American Meteorological Society*, *77*(3), 437–471. https://doi.org/10.1175/1520-0477(1996)077<0437:TNYRP>2.0

Kelley, M. C., Ilma, R. R., & Crowley, G. (2009). On the origin of pre-reversal enhancement of the zonal equatorial electric field. *Annales de Geophysique*, *27*(5), 2053–2056. https://doi.org/10.5194/angeo-27-2053-2009

Korenkov, Y. N., Klimenko, V. V., Klimenko, M. V., Bessarab, F. S., Korenkova, N. A., Ratovsky, K. G., et al. (2012). The global thermospheric and ionospheric response to the 2008 minor sudden stratospheric warming event. *Journal of Geophysical Research*, *117*(A10), A10309. https://doi.org/10.1029/2012JA018018

Laskar, F. I., Pallamraju, D., & Veenadhari, B. (2014). Vertical coupling of atmospheres: Dependence on strength of sudden stratospheric warming and solar activity. *Earth Planets and Space*, *66*, 1–10. https://doi.org/10.1186/1880-5981-66-94

Laštovička, J. (2006). Forcing of the ionosphere by waves from below. *Journal of Atmospheric and Solar-Terrestrial Physics*, *68*(3–5), 479–497. https://doi.org/10.1016/j.jastp.2005.01.018

Lin, C. H., Lin, J. T., Chang, L. C., Liu, J. Y., Chen, C. H., Chen, W. H., et al. (2012). Observations of global ionospheric responses to the 2009 stratospheric sudden warming event by FORMOSAT-3/COSMIC. *Journal of Geophysical Research*, *117*(6), 1–16. https://doi.org/10.1029/2011JA017230

Liu, H., Doornbos, E., Yamamoto, M., & Tulasi Ram, S. (2011). Strong thermospheric cooling during the 2009 major stratosphere warming. *Geophysical Research Letters*, *38*(12), L12102. https://doi.org/10.1029/2011GL047898

Liu, H., Jin, H., Miyoshi, Y., Fujiwara, H., & Shinagawa, H. (2013). Upper atmosphere response to stratosphere sudden warming: Local time and height dependence simulated by GAIA model. *Geophysical Research Letters*, *40*, 635–640. https://doi.org/10.1002/grl.50146

Liu, H.-L., & Roble, R. G. (2002). A study of a self-generated stratospheric sudden warming and its mesospheric-lower thermospheric impacts using the coupled TIME-GCM/CCM3. *Journal of Geophysical Research*, *107*(D23). ACL 15–1–ACL 15–18. https://doi.org/10.1029/2001jd001533

Matsuno, T. (1971). A dynamical model of the stratospheric sudden warming. *Journal of the Atmospheric Sciences*, *28*(8), 1494. https://doi.org/10.1175/1520-0469

Maute, A., Hagan, M. E., Yudin, V., Liu, H. L., & Yizengaw, E. (2015). Causes of the longitudinal differences in the equatorial vertical E × B drift during the 2013 SSW period as simulated by the TIME-GCM. *Journal of Geophysical Research—A: Space Physics*, *120*(6), 5117–5136. https://doi.org/10.1002/2015JA021126

Meyer Christian, K. (1999). Gravity wave interactions with the diurnal propagating tide. *Journal of Geophysical Research*, *104*(D4), 4223–4239. https://doi.org/10.1029/1998jd200089

Nishida, A. (1968). Coherence of geomagnetic DP2 magnetic fluctuations with interplanetary magnetic variations. *Journal of Geophysical Research*, *73*(17), 5549–5559. https://doi.org/10.1029/ja073i017p05549

Paes, R. R., Batista, I. S., Candido, C. M. N., Jonah, O. F., & Santos, P. C. P. (2014). Equatorial ionization anomaly variability over the Brazilian region during boreal sudden stratospheric warming events. *Journal of Geophysical Research: Space Physics*, *119*(9), 7649–7664. https://doi.org/10.1002/2014JA019968

Pedatella, N. M., Fang, T.-W., Jin, H., Sassi, F., Schmidt, H., Chau, J. L., et al. (2016). Multimodel comparison of the ionosphere variability during the 2009 sudden stratosphere warming. *Journal of Geophysical Research: Space Physics*, *121*(7), 7204–7225. https://doi.org/10.1002/2016JA022859

Pedatella, N. M., Forbes, J. M., Lei, J., Thayer, J. P., & Larson, K. M. (2008). Changes in the longitudinal structure of the low-latitude ionosphere during the July 2004 sequence of geomagnetic storms. *Journal of Geophysical Research*, *113*(A11), A11315. https://doi.org/10.1029/2008JA013539

Pedatella, N. M., & Liu, H.-L. (2018). The influence of internal atmospheric variability on the ionosphere response to a geomagnetic storm. *Geophysical Research Letters*, *45*(10), 4578–4585. https://doi.org/10.1029/2018gl077867

Ribeiro, B. A. G., Fagundes, P. R., Venkatesh, K., Tardelli, A., Pillat, V. G., & Seemala, G. K. (2019). Equatorial and low-latitude positive ionospheric phases due to moderate geomagnetic storm during high solar activity in January 2013. *Advances in Space Research*, *64*(4), 995–1010. https://doi.org/10.1016/j.asr.2019.05.032

Richmond, A. D., & Lu, G. (2000). Upper-atmospheric effects of magnetic storms: A brief tutorial. *Journal of Atmospheric and Solar-Terrestrial Physics*, *62*(12), 1115–1127. https://doi.org/10.1016/S1364-6826(00)00094-8

Rishbeth, H., Muller-Wodarg, I. C. F., Zou, L., Fuller-Rowell, T. J., Millward, G. H., Moffett, R. J., et al. (2000). Annual and semiannual variations in the ionospheric F2-layer: II. Physical discussion. *Annales de Geophysique*, *18*(8), 945–956. https://doi.org/10.1007/s00585-000-0945-6

Roble, R. G., Dickinson, R. E., & Ridley, E. C. (1982). Global circulation and temperature structures of thermosphere with high-latitude plasma convection. *Journal of Geophysical Research*, *87*(A3), 1599–1614. https://doi.org/10.1029/ja087ia03p01599

Siddiqui Tarique, A., Maute, A., Pedatella, N., Yamazaki, Y., Hermann, L., & Stolle, C. (2018). On the variability of the semidiurnal solar and lunar tides of the equatorial electrojet during sudden stratospheric warmings. *Annales de Geophysique*, *36*(6), 1545–1562. https://doi.org/10.5194/angeo-36-1545-2018

Sridharan, S., Sathishkumar, S., & Gurubaran, S. (2009). Variabilities of mesospheric tides and equatorial electrojet strength during major stratospheric warming events. *Annales de Geophysique*, *27*, 4125–4130. https://doi.org/10.5194/angeo-27-4125-2009. Retrieved from www.ann-geophys.net/27/4125/2009/

Tsurutani, B. T., Verkhoglyadova, O. P., Mannucci, A. J., Saito, A., Araki, T., Yumoto, K., et al. (2008). *Prompt penetration electric fields (PPEFs) and their ionospheric effects during the great magnetic storm of 30–31 October 2003*, 113(A5). https://doi.org/10.1029/2007ja012879

Vasyliunas, V. M. (1970). Mathematical models of magnetospheric convection and its coupling to the ionosphere. In M. McCormac (Ed.), (Ed). *Particles and fields in the magnetosphere* (pp. 60–71). Springer.

Vasyliunas, V. M. (1972). The interrelationship of magnetospheric processes. In B. M. McCormac (Ed.), *Earth's magnetosphere processes* (pp. 29–38). D. Reidel.

Venkatesh, K., Ram, S. T., Fagundes, P. R., Seemala, G. K., & Batista, I. S. (2017). Electrodynamic disturbances in the Brazilian equatorial and lowlatitude ionosphere on St. Patrick's Day storm of 17 March 2015. *Journal of Geophysical Research: Space Physics*, *122*(4), 4553–4570. https://doi.org/10.1002/2017JA024009

Yamazaki, Y., Yumoto, K., McNamara, D., Hirooka, T., Uozumi, T., Kitamura, K., et al. (2012). Ionospheric current system during sudden stratospheric warming events. *Journal of Geophysical Research*, *117*(3), 1–7. https://doi.org/10.1029/2011JA017453